

Original Article

Cite this article: Lloyd JC, Preiss WV, Collins AS, Virgo GM, Blades ML, Gilbert SE, Subarkah D, Krapf CBE, and Amos KJ. Geochronology and formal stratigraphy of the Sturtian Glaciation in the Adelaide Superbasin. *Geological Magazine* <https://doi.org/10.1017/S0016756823000390>

Received: 3 December 2022

Revised: 9 June 2023

Accepted: 21 June 2023







Keywords:

detrital zircon; geochronology; Sturtian; stratigraphy; provenance; tectonics; Rb-Sr geochronology

Corresponding author: Jarred C. Lloyd;

Email: jarredclloyd@gmail.com

Geochronology and formal stratigraphy of the Sturtian Glaciation in the Adelaide Superbasin

Jarred C. Lloyd^{1,2} , Wolfgang V. Preiss^{1,2}, Alan S. Collins¹ , Georgina M. Virgo¹, Morgan L. Blades¹ , Sarah E. Gilbert³ , Darwinaji Subarkah¹ , Carmen B.E. Krapf² and Kathryn J. Amos¹ 

¹School of Physics, Chemistry and Earth Sciences, University of Adelaide, Adelaide, SA 5005, Australia; ²Department for Energy and Mining, Geological Survey of South Australia, Adelaide, SA 5000, Australia and ³Adelaide Microscopy, University of Adelaide, Adelaide, SA 5005, Australia

Abstract

The glaciogenic nature of the Yudnamutana Subgroup was first recognized over a century ago, and its global significance was recognized shortly after, with the eventual postulation of a global Sturtian Glaciation and Snowball Earth theory. Much debate on the origin and timing of these rocks, locally and globally, has ensued in the years since. A significant corpus of research on the lithology, sedimentology, geochronology and formal lithostratigraphy of these sequences globally has attempted to resolve many of these debates. In the type area for the Sturtian Glaciation, South Australia's Adelaide Superbasin, the lithostratigraphy and sedimentology are well understood; however, formal stratigraphic nomenclature has remained complicated and contested. Absolute dates on the stratigraphy are also extremely sparse in this area. The result of these longstanding issues has been disagreement as to whether the sedimentary rocks of the Yudnamutana Subgroup are truly correlative throughout South Australia, and if they were deposited in the same time span recently defined for Sturtian glacial rocks globally, c. 717 Ma to c. 660 Ma. This study presents a large detrital zircon study, summarizes and compiles existing global geochronology for the Sturtian Glaciation and revises the formal lithostratigraphic framework of the Yudnamutana Subgroup. We show equivalence of the rocks that comprise the revised Sturt Formation, the main glaciogenic unit of the Yudnamutana Subgroup, and that it was deposited within the time span globally defined for the Sturtian Glaciation.

1. Introduction

The Neoproterozoic is a pivotal time in Earth's history with significant changes to Earth systems. These changes led to the Phanerozoic world of extensive macroscopic mineralized life, significantly oxygenated atmosphere and hydrosphere and a climate devoid of extreme glaciations of near-equatorial extent (Halverson *et al.* 2009; Och & Shields-Zhou, 2012; Wallace *et al.* 2017; Tostevin & Mills, 2020; Shields *et al.* 2022). Within the Neoproterozoic, the Cryogenian Period (derived from the Greek words κρύος and γένεση; meaning cold and birth, respectively), is named for the globally distributed and long-lasting continental glaciations characteristic of this time (Plumb & James, 1986; Plumb, 1991; Shields *et al.* 2018). The record of these glaciations is known on every continent except Antarctica (Arnaud *et al.* 2011), with notably well-studied sections in Australia. While the concept of globally distributed glaciations, and even the glaciogenic nature of some of these formations remains contentious (e.g., Eyles & Januszczak, 2004; Allen & Etienne, 2008; Williams & Gostin, 2019; Le Heron *et al.* 2020), most authors accept that at least two major glacial events are observed within Cryogenian rocks: an older Sturtian Glaciation and a younger Marinoan (also known as 'Elatina') Glaciation (or 'cryochron'; Hoffman *et al.* 2017). These two major glacial events of the Cryogenian coincide with major reorganizations of the biosphere (i.e. the rise of algae and other eukaryotic life, leading to the emergence of animals) (Brocks, 2018; Lechte *et al.* 2019).

Absolute geochronological constraints have become well established in several regions (Rooney *et al.* 2015) and are ever improving across the globe (e.g. Nascimento *et al.* 2017; MacLennan *et al.* 2018; Park *et al.* 2019; Rud'ko *et al.* 2020; Środoń *et al.* 2022). One notable exception is that of the sequences of Australia where some of the thickest and best-preserved Cryogenian glaciogenic formations are found. Until recently (Rose *et al.* 2013; Cox *et al.* 2018b; Keeman *et al.* 2020; Lloyd *et al.* 2020), radiometric dates of any form for the Cryogenian glaciogenic and intervening non-glacial sequences of the Adelaide Superbasin, South Australia, were extremely sparse (Ireland *et al.* 1998; Fanning & Link, 2006; Kendall *et al.* 2006). This is due, in part, to the dearth of known volcanogenic horizons within the South Australian Cryogenian sequences, the challenges of dating Precambrian sedimentary rocks

© The Author(s), 2023. Published by Cambridge University Press. This is an Open Access article, distributed under the terms of the Creative Commons Attribution licence (<http://creativecommons.org/licenses/by/4.0/>), which permits unrestricted re-use, distribution and reproduction, provided the original article is properly cited.



(Halverson *et al.* 2018; Shields *et al.* 2022), and the general lack of geochronological research conducted on the basin since the marked advancement in laser ablation (LA) and chemical abrasion geochronological techniques during the mid-2000s (Mundil *et al.* 2004; Mattinson, 2005; Gehrels *et al.* 2008). In this study, we address this by presenting a new in-situ Rb–Sr shale age from the Sturt Formation, 1034 new U–Pb detrital zircon (DZ) analyses from 15 samples (Fig. 1) of the Yudnamutana Subgroup (Sturtian Glaciation), 59 new U–Pb DZ analyses from the Yancowinna Subgroup of New South Wales (interpreted as a correlative of the Yudnamutana Subgroup (Fig. 2)) and an additional 56 new U–Pb DZ analyses from the post-Sturtian Glaciation Serle Conglomerate. The purpose of this paper is to provide the geochronological framework for the Cryogenian rocks recording the Sturtian Glaciation within the Adelaide Superbasin.

2. Geological background

2.a. Adelaide Superbasin

The Adelaide Superbasin comprises several named basins and sub-basins that form a large, Neoproterozoic to middle Cambrian sedimentary system at the southeast margin of Proterozoic Australia. Formation of the Adelaide Superbasin initiated at c. 890–830 Ma as a result of the breakup of the Rodinia supercontinent (Powell *et al.* 1994; Preiss, 2000; Lloyd *et al.* 2022). The Adelaide Rift Complex is the largest and oldest of the basins within the Adelaide Superbasin and includes a number of extensional depocentres, including the Yudnamutana Trough (northern Flinders Ranges), Baratta Trough (Olary and eastern Flinders Ranges) and Torrowangee Trough of western New South Wales (Fig. 1). The rift complex is contiguous with the relatively undeformed rocks of the Torrens Hinge Zone, Stuart Shelf (Sprigg, 1952) and Coomalarnie Platform (Callen, 1990). The Cambrian Arrowie Basin and Stansbury Basin are considered part of the Adelaide Superbasin (Preiss *et al.* 2002; Lloyd *et al.* 2020). Deposition within the Adelaide Superbasin occurred over a duration of ~300 Ma and stretched from the northernmost regions of South Australia to Kangaroo Island in the south, and east into western Victoria and New South Wales. The superbasin began as an intracontinental rift system that progressed to a passive margin system in the southeast and eastern parts of the basin, yet remained a failed rift in the north (Preiss, 2000; Lloyd *et al.* 2022). The cessation of the Adelaide Superbasin is marked by the Delamerian Orogeny c. 514–490 Ma (Drexel & Preiss, 1995; Preiss, 2000; Foden *et al.* 2006; Foden *et al.* 2020). Present day outcrop of the superbasin is largely restricted to the Flinders and Mount Lofty Ranges of South Australia, and the Barrier Ranges of South Australia and New South Wales.

The stratigraphy of the Adelaide Superbasin is divided into three supergroups, two of which are Neoproterozoic and the third is Cambrian (Preiss, 2000). The three supergroups are divided into numerous groups and subgroups (Fig. 2). The Warrina Supergroup is the oldest and comprises the Callanna, Burra and Poolamacca groups. The Heysen Supergroup contains the Umberatana, Wilpena, Torrowangee and Farnell groups. The Moralana Supergroup is the youngest and includes all the Cambrian sequences within the Adelaide Superbasin. In this paper, we focus on the lowermost division of the Umberatana Group, the Yudnamutana Subgroup (Figs. 2, 3), which comprises sedimentary rocks that represent the Sturtian Glaciation. Additional samples come from the overlying Nepouie

Subgroup and the Yancowinna Subgroup (New South Wales) which has been interpreted as a correlative of the Yudnamutana Subgroup (Fig. 2) (Cooper *et al.* 1974; Preiss, 1987).

The reader is referred to Preiss (1987), Preiss (2000), Counts (2017), Cowley (2020), Lloyd *et al.* (2020) and references therein for further detail on the geological history of the Adelaide Superbasin.

2.a.1. Yudnamutana Subgroup

The glaciogenic nature of rocks within the Yudnamutana Subgroup was first recognized by Howchin (1901), with those sequences being traced throughout the Mount Lofty, Flinders and Olary Ranges during the early 20th century (Preiss *et al.* 2011). Of particular note are the Yudnamutana Subgroup ‘tillites’ that rose to international prominence at the start of the 1900s (David, 1906; Howchin, 1908; Cooper, 2010 and references therein). As a result, a significant amount of research on the nature of the Yudnamutana Subgroup has been published over the past century (e.g. Howchin, 1901; Howchin, 1904; David, 1906; Howchin, 1906; Howchin, 1908; Howchin, 1920; Segnit, 1939; Mawson & Sprigg, 1950; Sprigg, 1952; Thomson *et al.* 1964; Forbes & Cooper, 1976; Coats & Forbes, 1977; Preiss *et al.* 1978; Link & Gostin, 1981; Preiss, 1987; Preiss *et al.* 1998; Preiss, 2000; Fanning & Link, 2008; Le Heron *et al.* 2011; Preiss *et al.* 2011; Cox *et al.* 2013; Le Heron *et al.* 2014; Cox *et al.* 2018b; Conor & Preiss, 2019; Virgo *et al.* 2021).

The Fitton Formation (Figs. 3, 4) is the oldest known unit of the Yudnamutana Subgroup and is present only in the Yudnamutana Trough of the northern Flinders Ranges (Fig. 1). The Fitton Formation consists of a basal conglomeratic facies, known as the Hamilton Creek Member, while the remainder of the formation is predominantly finely laminated mudstone and hornfels. The Hamilton Creek Member comprises laminated silty mudstone interbedded with gravel to boulder conglomerates and minor sandstone. The conglomerates range from a few centimetres to 20 m in thickness and are mostly massive although some have crude stratification. Sandy orthoconglomerates predominate, some are graded, with diamictite present in the lower parts of the unit. Mudstones are commonly interbedded with thin sandstone layers and gravel-to-pebble conglomerate. Some rare ripple-cross laminations are present in the unit, and dropstones are noted in the upper part of the member (Young & Gostin, 1989b). The majority of the Fitton Formation primarily comprises laminated silty mudstones containing abundant metamorphic scapolite, with diamictite beds throughout. Minor conglomerates, sandstones and actinolitic marbles are also present. Sandstones are more abundant in the lower half of the formation, while diamictite is more abundant in the upper half, as are dropstones (Preiss, 1987; Young & Gostin, 1989b). The formation has been interpreted as recording a sequence of glacial advance, retreat and then a second advance (Young & Gostin, 1989b). The Fitton Formation is conformably overlain by the Bolla Bollana Tillite (Young & Gostin, 1989b; Preiss *et al.* 1998).

The Bolla Bollana Tillite is one of six formally named diamictite-abundant formations of the Yudnamutana Subgroup, which are lithostratigraphic correlatives (Figs. 3, 5). The six correlative formations are the Appila Tillite (Thomson *et al.* 1964) (based on the section of Segnit, 1939), the Bolla Bollana Tillite (Thomson *et al.* 1964; Coats & Forbes, 1977), the Calthorinna Tillite (Ambrose *et al.* 1981), the Merinjina Tillite (Coats & Preiss, 1987), the Pualco Tillite (Forbes & Cooper, 1976) and the Sturt Tillite (Howchin, 1920; Mawson & Sprigg, 1950). These six correlative formations are here combined and referred to as the

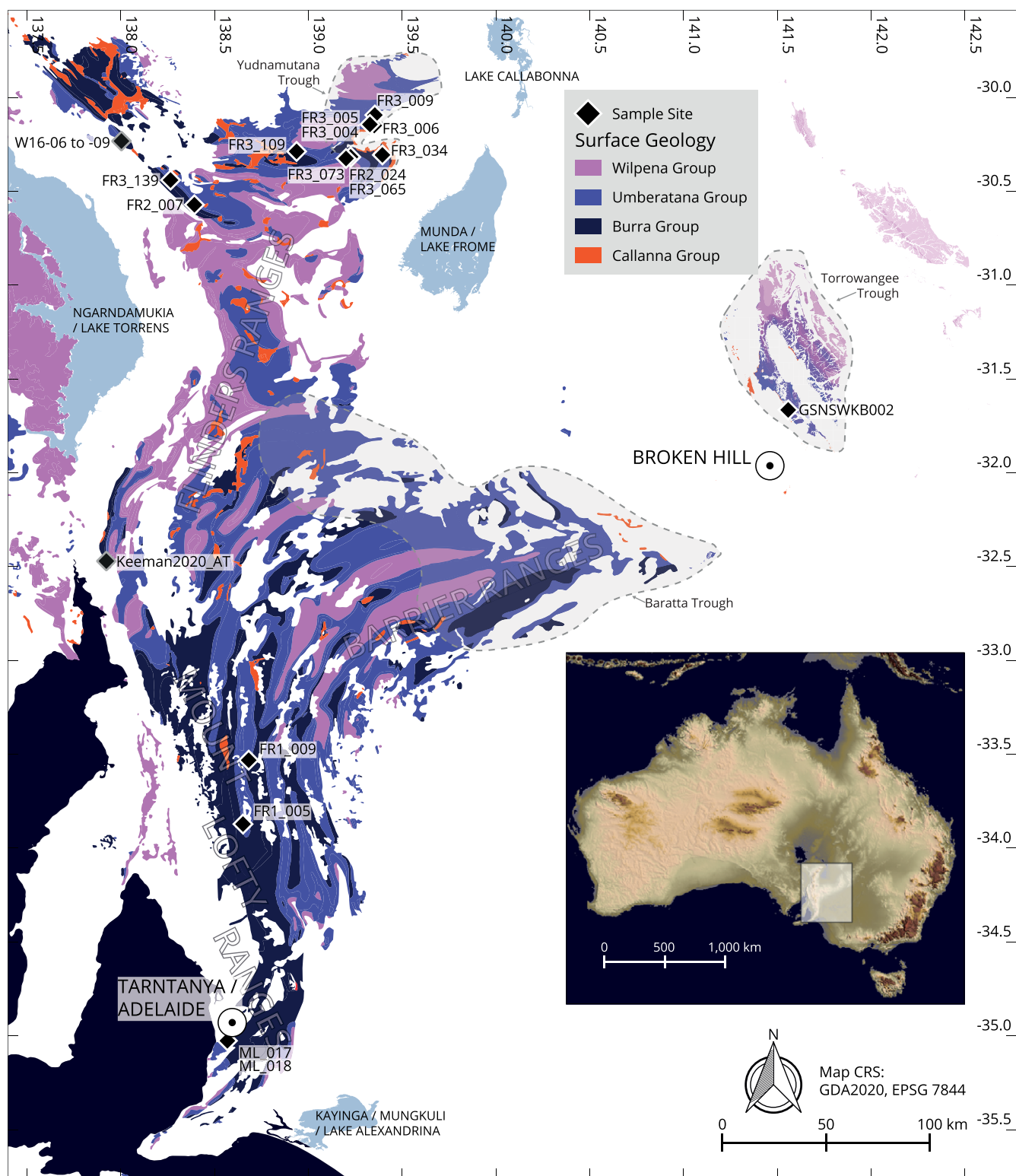


Figure 1. (Colour online) Sample locality map, showing distribution of Neoproterozoic stratigraphy within the Adelaide Rift Complex of the Adelaide Superbasin and Koonenberry Belt of New South Wales. GPS coordinates for samples are provided with the U-Pb data (see data availability). The Stuart Shelf lies to the east of Ngarndamukia/Lake Torrens, and the Davenport and Denison Ranges further to the northeast of the limit of this map.

Sturt Formation (Figs. 3, 5) with a formal redefinition presented in section 5.e.1 below.

At the type locality, the Sturt Formation comprises (boulder) diamictite showing evidence for glaciogenic origin and numerous subsidiary lithologies including poorly sorted sandstones and

conglomerates through to finely laminated shales containing a wide variety of limestones and dropstones (Fig. 4). Four generalized lithofacies are defined at the type location (Belperio, 1973; Young & Gostin, 1989b). The lowermost unit comprises very poorly sorted conglomerates with sandy matrix to diamictites with

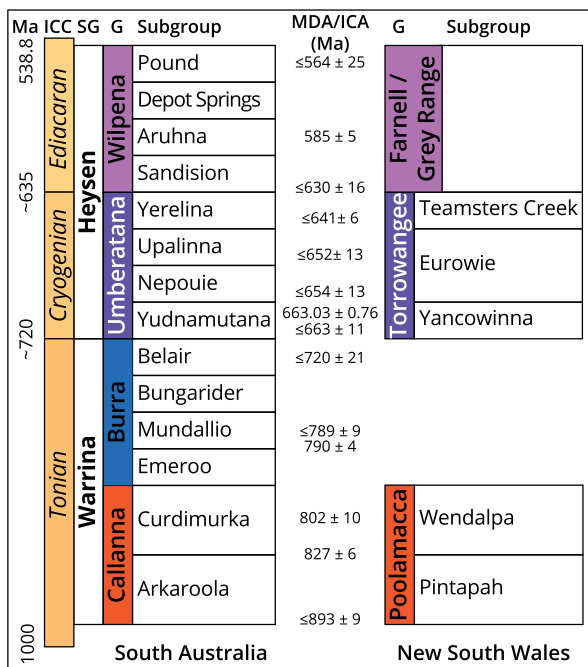


Figure 2. (Colour online) Simplified stratigraphic chart showing Supergroup, Group and Subgroup division of the Neoproterozoic stratigraphy within the Adelaide Superbasin. ICC = International chronostratigraphic chart; SG = Supergroup; G = Group; MDA/ICA = maximum depositional age (denoted by \leq) and igneous crystallization age (no preceding annotation). Colours used to fill group level cell are consistent with colours used in later figures. Geochronology data from Lloyd *et al.* (2020) and references therein, van der Wolff (2020), and Lloyd *et al.* (2022).

muddy, silty and even very fine sandy matrix. Clasts range up to boulder size (largest observed is ~ 1 m) and there are minor interbeds of laminated siltstone. A higher concentration of larger clasts is present in the lower sections. The next lithofacies comprises interbedded, well-laminated shales and sandy micaceous siltstones. There are minor pebbly lenses and silty arenites with cross-bedding present and are often ripple marked. The third lithofacies comprises crudely stratified diamictite (lithic wacke, muddy to silty matrix) with clasts ranging up to boulder size (max. observed: 90 cm). There are minor interbeds of calcareous shale and thick interbeds of massive diamictite. The uppermost lithofacies is similar to the third; however, it has a higher mud content in the matrix and is mostly massive diamictite. There are also a greater number of clasts with greater size diversity ranging up to 1.25 m (observed) in this uppermost lithofacies.

In general, the lithologic sequence common throughout the basin for the Sturt Formation (Fig. 5) for complete or near-complete sections consists of three units. The lowermost is a poorly sorted, gravel-to-boulder conglomerate (diamictite in some areas) with a generally sandy matrix. Scoured bases are common in areas where the Fitton Formation is not present. The middle unit comprises interbedded fine laminated siltstones and shales to cross-bedded sandstones with few limestones/dropstones. The uppermost unit is either a massive or stratified boulder diamictite. Regional variation does occur, notably arkosic, poorly sorted immature sandstones and cross-bedded sandstones are predominant in some areas. Carbonate matrixes and interbeds are abundant in some regions (Hood *et al.* 2021). Clast size and type in diamictite vary greatly across the basin, with sizes up to boulder megaclasts of ~ 1.25 km (Conor & Preiss, 2019). Iron-rich sections

are present within the Sturt Formation underlying the Benda Siltstone and Holowilena Ironstone (Preiss, 1987; Preiss *et al.* 2011; Lechte & Wallace, 2015).

The Benda Siltstone, Old Boolcoomata Conglomerate Member and Holowilena Ironstone either overlie or form the Sturt Formation (Fig. 3) but are only found in the Baratta Trough (Fig. 1) (Preiss, 2006; Lechte & Wallace, 2015; Conor & Preiss, 2019). The accurate stratigraphic correlation of these units is still uncertain; however, they are likely partial equivalents of both underlying (Sturt Formation) and overlying (Wilyerpa and Lyndhurst formations) stratigraphy. The Benda Siltstone and Holowilena Ironstone have complex interfingering stratigraphic relationships with the Sturt Formation and Wilyerpa Formation.

The Benda Siltstone comprises dark-weathering, calcareous, dark and medium grey laminated siltstone and minor silty limestone. Iron-rich siltstone occurs in the lower part of the Benda Siltstone. Regional variation includes interbedded sandstones and dolostones (Preiss, 1987). The Old Boolcoomata Conglomerate Member of the Benda Siltstone comprises mainly clast-supported oligomictic conglomerate and minor arkosic grit. Clasts in the Old Boolcoomata Conglomerate Member are predominantly well-rounded to subrounded and mainly consist of two-mica S-type granites from the early Mesoproterozoic Bimbrowie Suite, with subsidiary clasts of migmatite, psammite, psammopelite, pelitic schist, albistized metasediment and calclbitite (Preiss, 2006).

The Holowilena Ironstone is defined as a haematite siltstone with lenses of dolomite and wacke with glacial erratics and is considered to be an unmetamorphosed equivalent of the Benda Siltstone (Thomson *et al.* 1964; Preiss, 1987, 1993). The Holowilena Ironstone comprises hematitic siltstone, siltstone with minor lenses of dolomite, quartzite and pebbly to boulder, often massive ironstone (Thomson *et al.* 1964; Preiss, 1987; Lechte & Wallace, 2015). The silty units are thinly and evenly bedded, occasionally with small cross-bedding. Regionally, some jasper is present.

The Wilyerpa Formation (Thomson *et al.* 1964; Dalgarno & Johnson, 1966; Forbes, 1971) and correlative Lyndhurst Formation (Figs. 3, 4) (Thomson *et al.* 1964; Young & Gostin, 1989b) are the youngest units of the Yudnamutana Subgroup (Fig. 2) and have been interpreted to represent the waning of the Sturtian Glaciation (Preiss, 1987; Preiss *et al.* 1998; Cox *et al.* 2018b).

The Wilyerpa Formation is a variably thick unit (up to 4,400 m) comprising grey to green siltstones and shales with interbedded arenites and subsidiary diamictites and dolostones. Arkosic and quartzitic sandstones are common and predominate in some areas (Preiss, 1987). Two members, the Warcowie Dolomite Member and Bibliando Tillite Member, are defined within the Wilyerpa Formation. While originally thought to be restricted to the Baratta Trough (Fig. 1), subsequent research indicates that the Wilyerpa Formation may be more widespread (Fanning & Link, 2006; Fanning & Link, 2008; Cox *et al.* 2018b). Relationships with the underlying stratigraphy (Sturt Formation, Benda Siltstone, Holowilena Ironstone) are variable with some areas being gradational and others disconformable, the latter likely due to active tectonics (Preiss, 1987; Preiss *et al.* 1998; Preiss, 2000).

The Lyndhurst Formation is a sequence of predominantly laminated and ripple cross-laminated, blue pyritic and silty shale with minor green silty shale and interbedded quartzite, grits and sparse pebbly diamictites (Fig. 4). The unit conformably overlies the Sturt Formation and is considered to be restricted to the Yudnamutana Trough (Fig. 1) (Preiss, 1987; Young & Gostin, 1989b; Preiss *et al.* 1998).

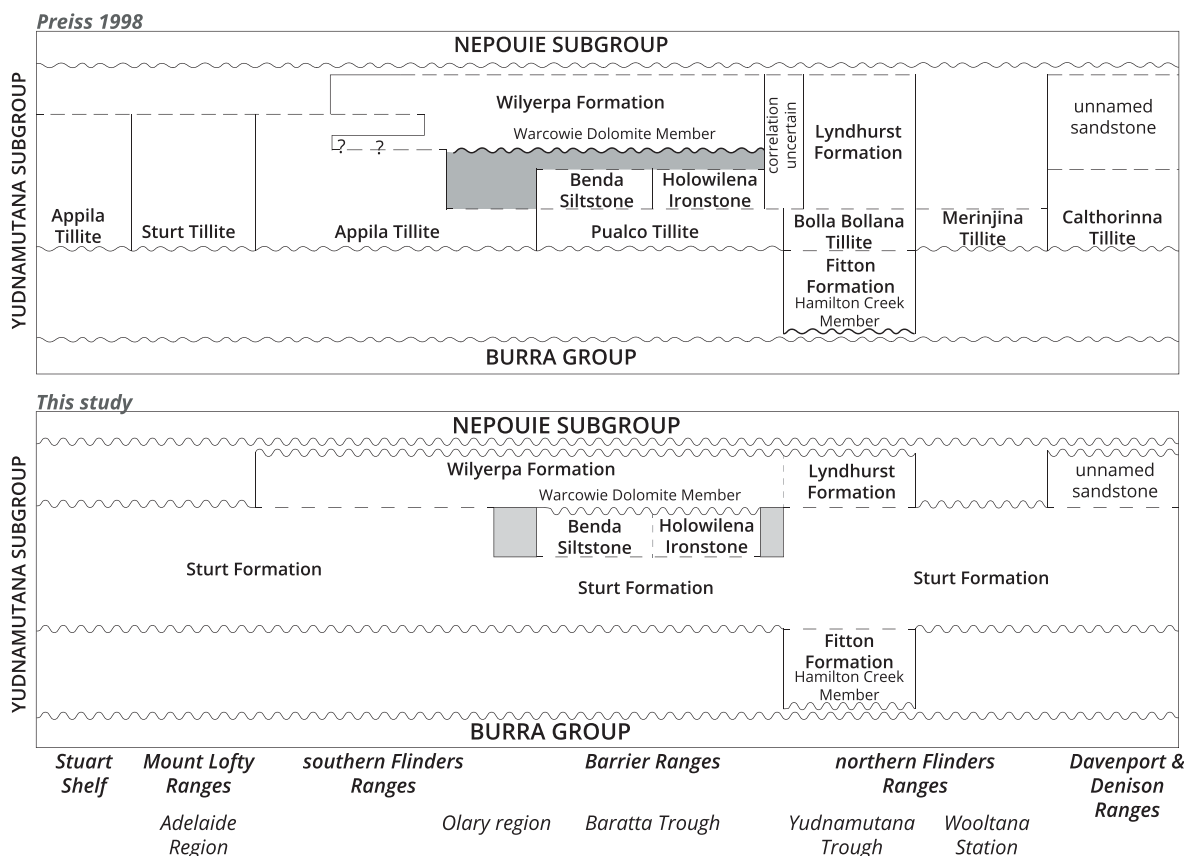


Figure 3. (Colour online) Stratigraphic table showing past (Preiss *et al.* 1998) and current correlations (this study) of the Yudnamutana Subgroup.

2.a.2. Yancowinna Subgroup

The Yancowinna Subgroup, Torrowangee Group, of western New South Wales was defined by Cooper and Tuckwell (1971) and described in more detail by Cooper *et al.* (1974). It consists of a sequence of coarse poorly sorted siliciclastics that include arkose, quartzite, sandstone, siltstone, conglomerate and diamictite (Cooper *et al.* 1974; Preiss, 1987; Fitzherbert & Downes, 2015). Tillite has only been confidently recognized in one area (Cooper, 1973), but many of the facies closely resemble probable correlatives (Fig. 2) in South Australia (Preiss, 1987).

The Yancowinna Subgroup is overlain by the Euriowie Subgroup (postglacial) that is in turn overlain by the Teamsters Creek Subgroup (Fig. 2), which has been interpreted as recording the younger Cryogenian Marinoan (Elatina) Glaciation (Preiss, 1987; Fitzherbert & Downes, 2015). The stratigraphic position of the Yancowinna Subgroup supports correlation with the Yudnamutana Subgroup of South Australia. Aside from detailed mapping and the original sedimentological work, there is extraordinarily little research on the Torrowangee Group (Fig. 2) sequences, and no geochronology has been published to date. As such the correlations are likely but uncertain and not yet confirmed by geochronology.

2.a.3. Nepouie Subgroup

The postglacial Nepouie Subgroup (Fig. 2) is believed to begin with the Serle Conglomerate, a sequence of stratified to crudely stratified conglomerates, with interbedded sandstones and shales (Young & Gostin, 1989a; Preiss *et al.* 1998). The conglomerates of the Serle Conglomerate trend from primarily sandy siliciclastic matrix to carbonate-rich matrix up-sequence and are interpreted

to have been deposited as part of a submarine fan complex (Young & Gostin, 1989a). The stratigraphic position of the Serle Conglomerate is still somewhat uncertain; however, it appears to conformably underlie the Tapley Hill Formation and unconformably overlie the Lyndhurst Formation (Fig. 3) with an erosional contact (Young & Gostin, 1989a; Dyson, 1996; Preiss *et al.* 1998; Dyson, 2004).

The Tapley Hill Formation primarily comprises well-sorted, commonly carbonaceous, calcareous or dolomitic siltstone, with pyritic shale and dolostone at its base (i.e. the Tindelpina Shale Member). Grain size and carbonate content tend to increase up-sequence, and fine laminations are abundant throughout the Tapley Hill Formation. While extensive in both distribution (basin-wide) and lithological uniformity, there are several minor lithofacies variations within the Tapley Hill Formation, including arkose, wacke, siltstone, dolostone and lenticular conglomerate beds (Preiss, 1987; Preiss *et al.* 1998; Virgo *et al.* 2021). The latter is attributed to debris flows reworking the underlying glaciogenic sequences (Preiss, 1987). Where the Serle Conglomerate is not present, the base of the Tapley Hill Formation is often disconformable with the underlying Yudnamutana Subgroup, although it may be gradational over a few centimetres in some areas (Preiss, 1987).

The youngest units of the Nepouie Subgroup are the Brighton Limestone and Balcanoona Formation, which conformably overlay and often interfinger with the Tapley Hill Formation. Both formations are predominately limestones with oolitic and stromatolitic features (Preiss, 1987, 2000). The Balcanoona Formation is coeval with the upper Tapley Hill Formation, forming large palaeo-reef systems above it and passing laterally

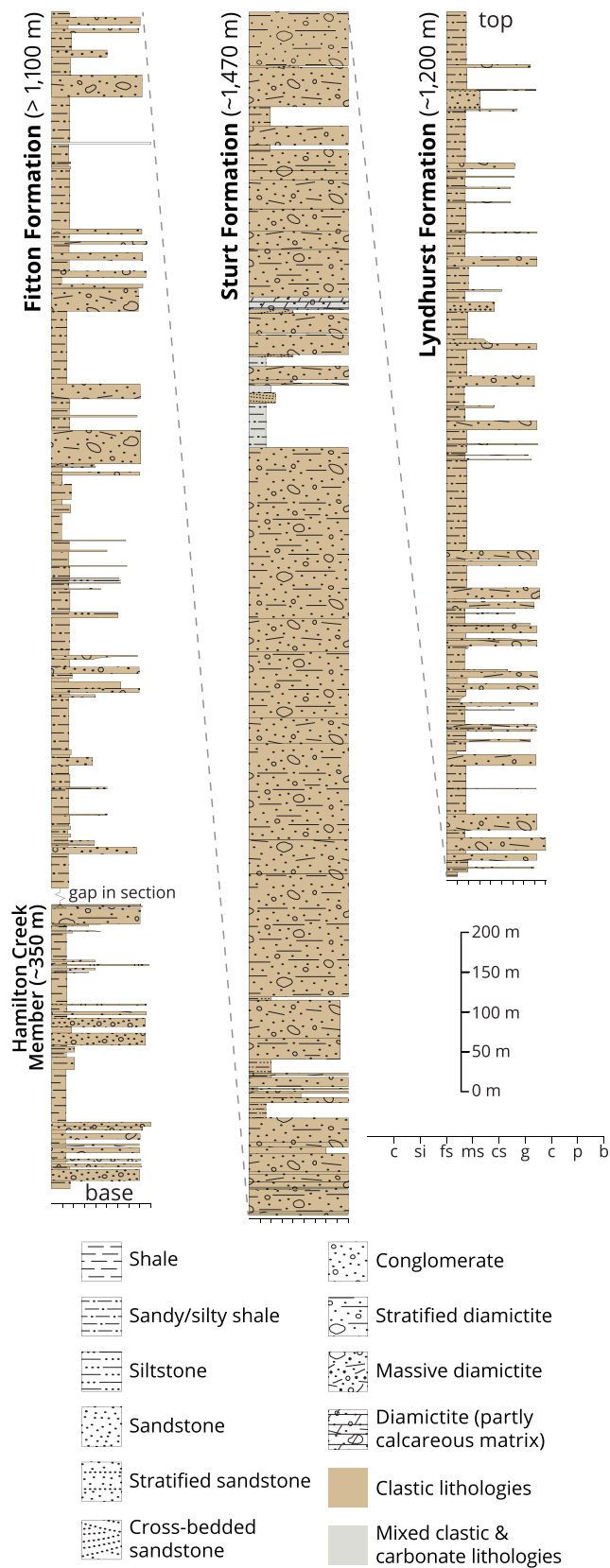


Figure 4. (Colour online) Generalized composite stratigraphic log of the Fitton Formation, Sturt Formation and Lyndhurst Formation at their type sections near MacDonal Creek, Arkaroola area. Based on data from Young and Gostin (1989b).

into it (Wallace *et al.* 2015), while the Brighton Limestone has been interpreted as the culmination of shallowing at the top of the Nepouie Subgroup (Preiss, 2000).

2.b. Sturtian Glaciation

The term Sturtian was originally defined as a chronostratigraphic unit (Series) in South Australia (Mawson & Sprigg, 1950) and was later proposed for use as a global chronostratigraphic division by Dunn *et al.* (1971). However, this archaic local chronostratigraphic terminology has been superseded by international nomenclature (Plumb, 1991; Gradstein *et al.* 2005; Knoll *et al.* 2006; Shields-Zhou *et al.* 2016; Shields *et al.* 2022). Presently, ‘Sturtian’ is used informally by the international community as the name for the older of two global (or near-global) glacial events proposed to have occurred during the Cryogenian (Harland, 1964; Kirschvink, 1992; Hoffman *et al.* 1998; Hoffman & Schrag, 2002; Fairchild & Kennedy, 2007; Hoffman *et al.* 2017). In a split from growing consensus, Le Heron *et al.* (2020) have advocated that the term ‘Laurentian Neoproterozoic Glacial Interval’ is used in favour of Sturtian, and that use of Sturtian should become restricted to the formations in Australia – a concept we are not in favour of and discuss in section 5.e.2 below.

The global distribution of Cryogenian glacial sequences, in particular those now attributed to the Sturtian Glaciation, was recognized nearly a century ago (Cooper, 2010; Hoffman, 2011; Hoffman *et al.* 2017 and references therein). However, their synchronicity was long debated until the advent of reliable and precise radiometric geochronology within the past two decades, which supports that, separately, the onset of glaciation and deglaciation of each of the two major Cryogenian glacial events (Sturtian and Marinoan Glaciations) is coeval globally (Fig. 6) (e.g., Dempster *et al.* 2002; Kendall *et al.* 2006; Kendall *et al.* 2009; Xu *et al.* 2009; Macdonald *et al.* 2010; Calver *et al.* 2013; Miller, 2013; Rooney *et al.* 2014; Rooney *et al.* 2015; Hoffman *et al.* 2017; Cox *et al.* 2018b; Shields *et al.* 2018; Lamothe *et al.* 2019; Park *et al.* 2019; Keeman *et al.* 2020; Lloyd *et al.* 2020; Rooney *et al.* 2020). This global synchronicity led Hoffman *et al.* (2017) to propose calling the Cryogenian glacial events ‘cryochrons’. For the older Sturtian event within the Cryogenian, the onsets of glaciation and deglaciation are interpreted to occur at c. 717 Ma at c. 660 Ma, respectively (Fig. 6) (Rooney *et al.* 2015; Hoffman *et al.* 2017).

Many of the thickest Cryogenian glacial successions are found in extensional basins associated with the break-up of Rodinia; the very thick Yudnamutana Subgroup (Figs. 2, 3) deposits in the Baratta, Yudnamutana and Torrowangee troughs (Fig. 1) of the Adelaide Superbasin are typical of these.

3. Methods

3.a. DZ U–Pb geochronology

Seventeen samples were analysed for DZ U–Pb geochronology; 15 diamictite samples (Fig. 1) from the Yudnamutana Subgroup (FR1_005_02, FR1_009_01, FR2_007_01, FR2_024_01, FR3_005, FR3_006, FR3_009, FR3_034, FR3_065, FR3_073, FR3_084a, FR3_109, FR3_139, ML_017 and ML_018), one diamictite sample from the correlative Yancowinna Subgroup (GSNSWK002), and one conglomerate sample from the lowermost Nepouie Subgroup (FR3_004). The distribution of these samples was intended to

Type and Reference Sections for the Sturt Formation, South Australia

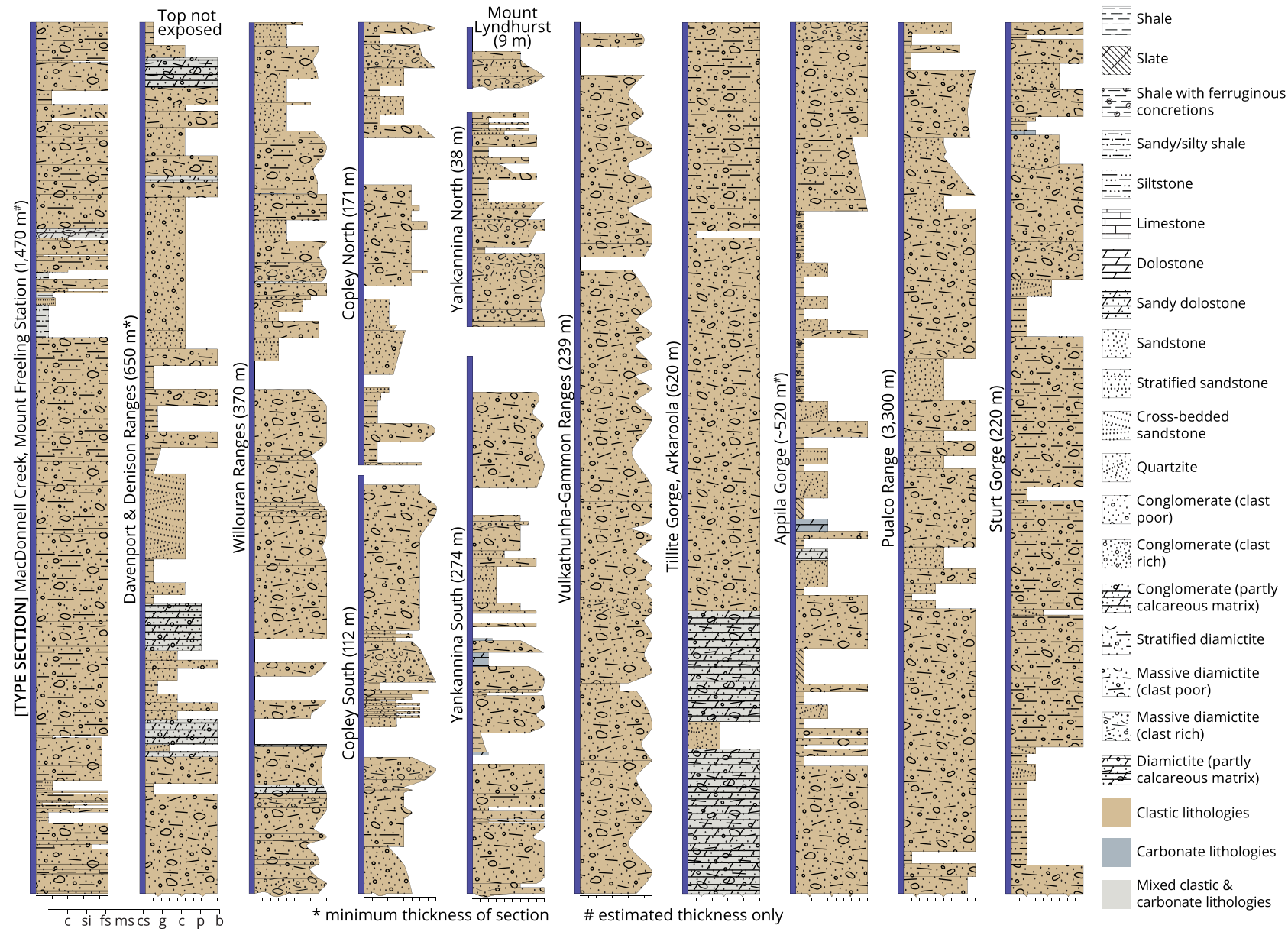


Figure 5. (Colour online) Generalized stratigraphic logs of the Sturt Formation at its type section and additional reference sections. For coordinates of locations see the accompanying stratigraphic unit definition (Appendix 2). Copley, Yankannina, Willouran Ranges and Vulkathuhna-Gammon Ranges sections are from logging done by authors in this study. Type section is based on data from Belperio (1973) and Young and Gostin (1989b). Other sections are compiled from Segnit (1939), Forbes and Cooper (1976), Coats and Preiss (1987) and Link (1977).

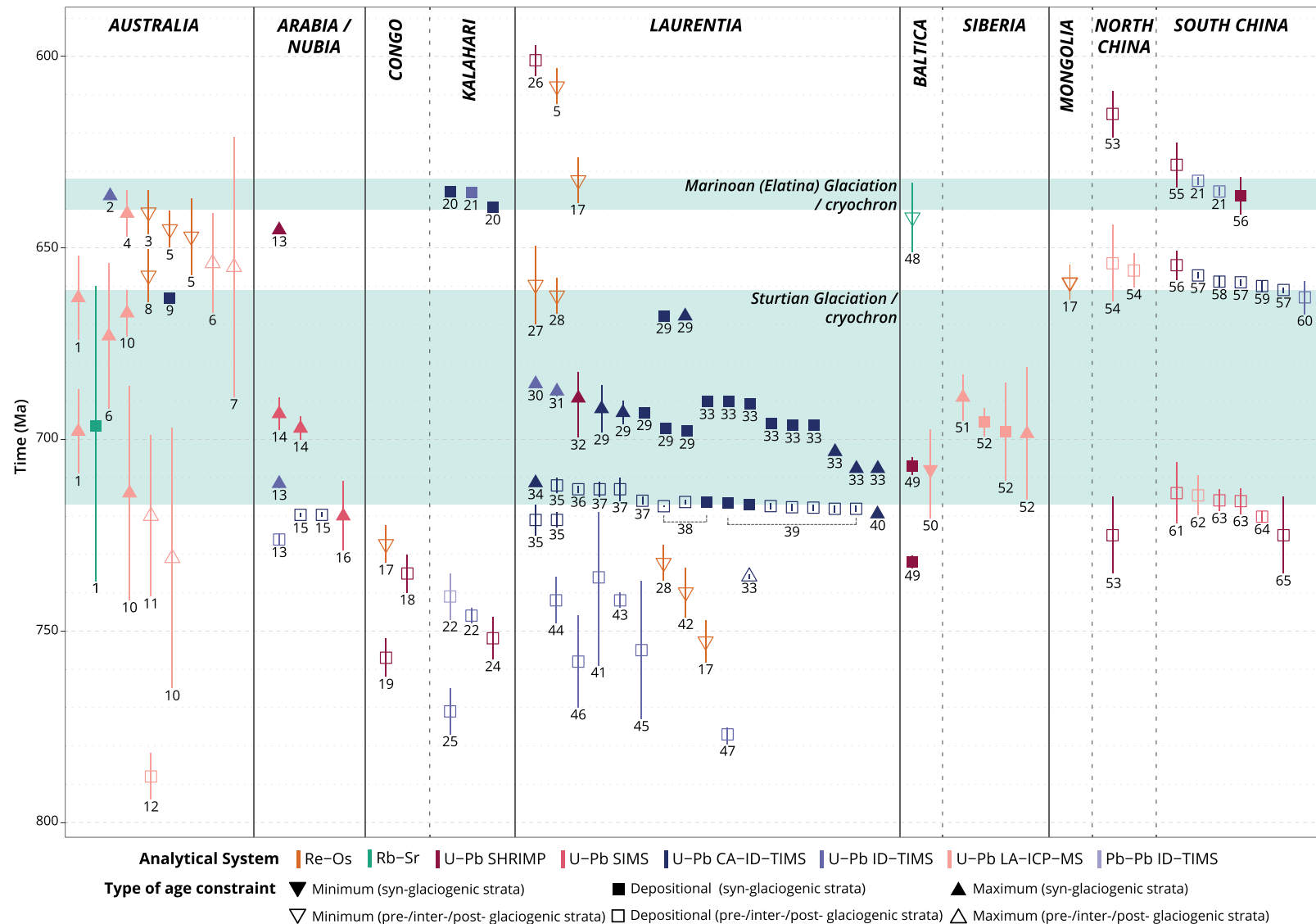


Figure 6. (Colour online) Compilation of global geochronologic data for the Sturtian and Marinoan (Elatina) Glaciations. Symbols are colour coded to reflect analytical method (see Fig. legend for details). Open symbols are data from pre-, inter- and post-glaciogenic strata, and closed symbols denote data from syn-glaciogenic strata. Shapes signify age type where squares are considered syn-depositional ages, and triangles denote minimum (tip points older) or maximum (tip points younger) depositional ages. Data sources: **AUSTRALIA:** (1) This study; (2) Calver *et al.* (2013); (3) Kendall *et al.* (2009); (4) Rose *et al.* (2013); (5) Kendall *et al.* (2004); (6) Lloyd *et al.* (2020); (7) Ireland *et al.* (1998); (8) Kendall *et al.* (2006); (9) Cox *et al.* (2018b); (10) Keeman *et al.* (2020); (11) van der Wolff (2020); (12) Armistead *et al.* (2020). **ARABIA/NUBIA:** (13) Bowering *et al.* (2007); (14) Abd El-Rahman *et al.* (2020); (15) MacLennan *et al.* (2018); (16) Li *et al.* (2018). **CONGO:** (17) Rooney *et al.* (2015); (18) Key *et al.* (2001); (19) Nascimento *et al.* (2016). **KALAHARI:** (20) Prave *et al.* (2016); (21) Schmitz (2012); (22) Frimmel *et al.* (1996); (23) Hoffman *et al.* (1996); (24) Borg *et al.* (2003); (25) Frimmel *et al.* (2001). **LAURENTIA:** (5) Kendall *et al.* (2004); (17) Rooney *et al.* (2015); (26) Dempster *et al.* (2002); (27) Rooney *et al.* (2011); (28) Rooney *et al.* (2014); (29) Isakson (2017); (30) Keeley *et al.* (2013); (31) Condon and Bowering (2011); (32) Lund *et al.* (2003); (33) Eyster *et al.* (2018); (34) Baldwin *et al.* (2016); (35) Denysyn *et al.* (2009); (36) Cox *et al.* (2018a); (37) Denysyn *et al.* (2009); (38) Macdonald *et al.* (2010); (39) Macdonald *et al.* (2018); (40) Cox *et al.* (2015); (41) McDonough and Parrish (1991); (42) Strauss *et al.* (2014); (43) Fetter and Goldberg (1995); (44) Karlstrom *et al.* (2000); (45) Ross and Villeneuve (1997); (46) Aleinikoff *et al.* (1995); (47) Jefferson and Parrish (1989). **BALTICA:** (48) Zaitseva *et al.* (2019); (49) Krasnobaev *et al.* (2019); (50) Śródoń *et al.* (2022). **SIBERIA:** (51) Kochnev *et al.* (2015); (52) Rud'ko *et al.* (2020). **MONGOLIA:** (17) Rooney *et al.* (2015). **NORTH CHINA:** (53) Xu *et al.* (2009); (54) He *et al.* (2014). **SOUTH CHINA:** (21) Schmitz (2012); (55) Chongyu *et al.* (2005); (56) Zhang *et al.* (2005); (57) Rooney *et al.* (2020); (58) Zhou *et al.* (2019); (59) Zhou *et al.* (2020); (60) Zhou *et al.* (2004); (61) Lan *et al.* (2015); (62) Song *et al.* (2017); (63) Lan *et al.* (2014); (64) Lan *et al.* (2020); (65) Zhang *et al.* (2008).

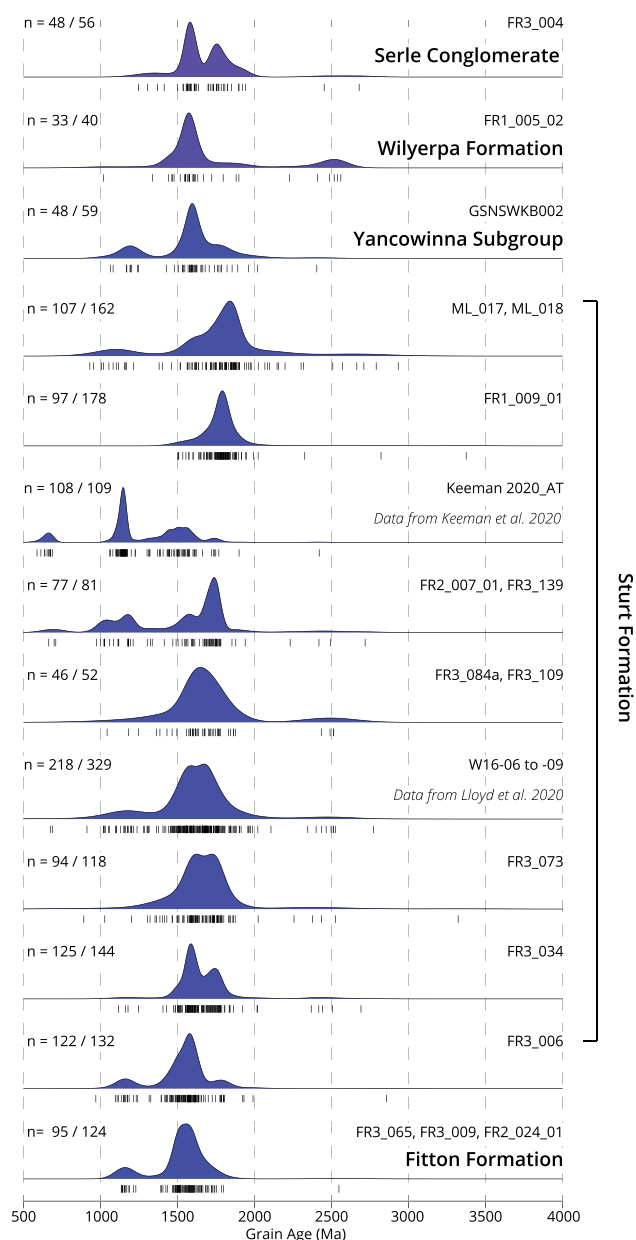


Figure 7. (Colour online) Kernel density estimates (KDEs) of detrital zircon populations from Yudnamutana, Yancowinna and Nepouie Subgroup samples. Data are from this study unless otherwise denoted. Tick marks below each plot represent an analysis. n = filtered analyses/total analyses. Generated using IsoplotR (Vermeesch, 2018).

provide good geographic and stratigraphic coverage across the basin system for strata of interest.

Rock samples were prepared for DZ analysis by standard methods at the University of Adelaide (Lloyd *et al.* 2022). Cathodoluminescence images were obtained on either a FEI Quanta 600 scanning electron microscope (for zircon analysed in 2020) or a Cameca SXFive Electron Microprobe (for zircon analysed in 2021). All zircons were analysed using a RESOLUTION-LR 193 nm ArF excimer LA system coupled with an Agilent 7900x inductively coupled plasma mass spectrometer (ICP-MS) to obtain a suite of elemental data for U–Pb geochronology and rare earth element analysis. All analytical instruments used are housed at Adelaide Microscopy, University of Adelaide, Australia.

Primary calibration reference materials were the zircon standard GJ-1 (Jackson *et al.* 2004; Horstwood *et al.* 2016) for U–Pb ratios, and the glass standard NIST610 (Jochum *et al.* 2011) for Pb isotope ratios and trace element data. Zircon standards Plešovice (Sláma *et al.* 2008; Horstwood *et al.* 2016) and 91500 (Wiedenbeck *et al.* 1995; Wiedenbeck *et al.* 2004; Horstwood *et al.* 2016) were used as validation reference materials to check accuracy. Data were processed using LADR (Norris & Danyushevsky, 2018), version 1.1.06. Statistical analysis of the zircon U–Pb data follows the method of Lloyd *et al.* (2020). Data are considered concordant if within $\pm 10\%$, and a *meaningful* age if the two-standard error (2SE) uncertainty is $\leq 10\%$ – if a datum satisfies both parameters it is termed a *Filtered Age*. Maximum depositional ages (MDAs) are determined from the youngest single grain (YSG); however, a stricter 2% concordance filter is used to determine a conservative and reliable MDA from the YSG. All uncertainties are quoted at 2SE level. Further details can be found in Appendix 1 (Extended Methods).

Metadata for the LA-ICP-MS sessions, data for all analyses, cathodoluminescence images and R code used to generate plots are available from the links in data and code availability.

3.b. In-situ Rb–Sr geochronology

Two siltstone/shale samples (3404236 and 3404235) were acquired for in-situ Rb–Sr geochronology from the Sturt Formation within drillhole SR13/2 located on the north-eastern margin of the Stuart Shelf, South Australia. Samples were mounted and polished as rock blocks in 25 mm round epoxy and then mapped for mineral composition and petrography using a Hitachi SU3800 SEM (Subarkah *et al.* 2021, 2022). Samples were analysed using an Agilent 8900x ICP-MS/MS coupled to a RESOLUTION-LR 193 nm ArF excimer LA system. All instruments are housed at Adelaide Microscopy, the University of Adelaide. Methods follow Redaa *et al.* (2021) and Subarkah *et al.* (2021). Primary calibration reference materials were NIST610 (Jochum *et al.* 2011) for Sr isotope ratios, and the Mica-Mg (Govindaraju, 1995) pressed nanopowder pellet for Rb–Sr ratios. Accuracy was checked by analysing MDC (crystalline phlogopite) and Högso (crystalline muscovite) (Hogmalm *et al.* 2017; Redaa *et al.* 2021) as validation reference materials. Data were reduced in LADR (Norris & Danyushevsky, 2018) version 1.1.07.

Isochrons were calculated using IsoplotR (Vermeesch, 2018) using a ^{87}Rb decay constant (λ) of $(1.3972 \pm 0.0045) \times 10^{-11} \text{ a}^{-1}$ (Villa *et al.* 2015). Error correlations (ρ) were calculated in LADR by using a workaround to proxy the Rb–Sr data as U–Pb data. Uncertainties are quoted at 2SE level (accounting for overdispersion), initially without decay constant uncertainty propagation. The decay constant uncertainty is propagated into the quoted 2SE uncertainty (accounting for overdispersion) during the discussion when compared to other geochronometric systems. Further details can be found in Appendix 1 (Extended Methods). The Rb–Sr data are available from the links provided in data availability.

4. Results

4.a. DZ geochronology

4.a.1. Fitton Formation

A total of 124 U–Pb and trace element DZ analyses were conducted for samples FR3_065 (92/74), FR3_009 (9/1) and FR2_024_01 (23/20), with 95 analyses passing filtering

parameters. Data from these samples were combined as only two samples yield more than one filtered analysis. The two samples with more than one filtered analysis were ~200 m apart (geographically), all three samples were from the broader local area (Fig. 1) and there were no discernible differences in the age spectra. Ages range from 2458 ± 37 Ma to 1134 ± 24 Ma, with a primary population peak c. 1580 Ma and a secondary peak c. 1160 Ma (Fig. 7).

4.a.2. Sturt Formation and equivalents

A total of 162 U–Pb and trace element DZ analyses were conducted for samples ML_017 (117/93) and ML_018 (45/14), South Mount Lofty Ranges (Sturt Gorge, Adelaide), with 107 analyses passing filtering parameters. Data from these samples were combined as the two sampling sites were ~60 m apart (geographically) (Fig. 1). Ages range from 2933 ± 34 Ma to 930 ± 16 Ma, with a primary population peak c. 1840 Ma, tailing towards 1560 Ma. A minor population peak is present c. 1100 Ma (Fig. 7).

A total of 178 U–Pb and trace element DZ analyses were conducted for sample FR1_009_01, North Mount Lofty Ranges (Spalding area) (Fig. 1), with 98 passing filtering parameters. Ages range from 3374 ± 32 Ma to 1501 ± 48 Ma, with a single population peak c. 1790 Ma (Fig. 7).

A total of 81 U–Pb and trace element DZ analyses were conducted for samples FR2_007_01 (31/28) and FR3_139 (50/49), North Flinders Ranges (Copley area) (Fig. 1), with 77 analyses passing filtering parameters. Data from these samples were combined for MDS and KDE analysis as they were sampled from the same stratigraphic interval (Fig. 1) at the approximately same stratigraphic position, and their age spectra are remarkably similar (Fig. 7). Ages range from 2718 ± 21 Ma to 663 ± 11 Ma, with a primary population peak c. 1740 Ma and secondary population peaks c. 1580 Ma, 1180 Ma and 1050 Ma (Fig. 7). The individual sample MDAs were 663 ± 11 Ma for FR3_139 and 698 ± 12 Ma for sample FR2_007_01.

A total of 52 U–Pb and trace element DZ analyses were conducted for samples FR3_084a (10/9) and FR3_109 (42/37), North Flinders Ranges (Yankaninna area), with 46 analyses passing filtering parameters. Data from these two samples were combined as they were sampled from within 30 m of each other in the same interval of outcrop (Fig. 1). Ages range from 2514 ± 48 Ma to 1042 ± 19 Ma, with a single population peak c. 1640 Ma (Fig. 7).

A total of 118 U–Pb and trace element DZ analyses were conducted for sample FR3_073, North Flinders Ranges (Vulkathuhna-Gammon Ranges) (Fig. 1), with 94 passing filtering parameters. Ages range from 3322 ± 35 Ma to 891 ± 15 Ma, with a single broad, and slightly bimodal population peak range of c. 1740 Ma to c. 1620 Ma (Fig. 7).

A total of 144 U–Pb and trace element DZ analyses were conducted for sample FR3_034, North Flinders Ranges (Stubbs Waterhole, Arkaroola), with 125 passing filtering parameters. Ages range from 2691 ± 42 Ma to 1117 ± 34 Ma, with a primary population peak c. 1590 Ma and a secondary population peak c. 175 Ma (Fig. 7).

A total of 132 U–Pb and trace element DZ analyses were conducted for sample FR3_006, North Flinders Ranges (Stanley Mine, Arkaroola) (Fig. 1), with 122 passing filtering parameters. Ages range from 2858 ± 47 Ma to 969 ± 16 Ma, with a primary population peak c. 1580 Ma and secondary population peaks c. 1790 Ma and 1160 Ma (Fig. 7).

A total of 59 U–Pb and trace element DZ analyses were conducted for sample GSNSWKB002, Yancowinna Subgroup, Barrier Ranges (New South Wales) (Fig. 1), with 48 passing filtering parameters. Ages range from 2404 ± 37 Ma to 1065 ± 18 Ma (Fig. 7).

4.a.3. Lyndhurst and Wilyerpa Formations

Sample FR3_005, Lyndhurst Formation, had extremely low zircon yield with only three zircons obtained and analysed for U–Pb ratios and trace element concentrations. Of those three zircon analyses, only two passed filtering parameters, with ages of 1532 ± 24 Ma and 1174 ± 19 Ma (Fig. 7).

A total of 40 U–Pb and trace element DZ analyses were conducted for sample FR1_005_02, Wilyerpa Formation, North Mount Lofty Ranges (Fig. 1). Of these 40 analyses, 33 passed filtering parameters with ages ranging from 2560 ± 79 Ma to 1020 ± 19 Ma, with a primary population peak c. 1580 Ma and a secondary population peak c. 2500 Ma (Fig. 7).

4.a.4. Serle Conglomerate

A total of 56 U–Pb and trace element DZ analyses were conducted for sample FR3_004, Serle Conglomerate, with 48 passing filtering parameters. Ages range from 2679 ± 65 Ma to 1246 ± 24 Ma, with a primary population peak c. 1590 Ma and a secondary population peak c. 1760 Ma (Fig. 7).

4.b. Zircon trace element geochemistry

Most analyses resolved lanthanoid concentrations that are typical for zircons, with several orders-of-magnitude increase in concentration from light to heavy elements, a slight negative deviation in europium (Eu) and a positive deviation in cerium (Ce) (Supplementary Figure S1). However, two analyses (FR1_009_01b-057 and FR1_009_01-044) have lanthanoid concentrations atypical of zircon, with overall positive (based on ionic radii) linear slopes (λ_1 of +7.14, and +1.06) due to highly elevated concentrations of light lanthanoids (La to Nd). Overall, the lanthanoid pattern of both analyses has a concave-up shape with heavy lanthanoid concentration increasing as would normally occur in zircon. Major element percentages, ~14.4 wt% and ~15.6 wt% silicon, suggest these two analyses are zircon, and CL images also support this, although show patchy textures. The ages for these are at the limit of discordance acceptance (90%). It is likely these two analyses have gone through complicated zones of inclusions, altered metamict zones and/or mineral overgrowths.

4.c. Shale petrology and in-situ Rb–Sr geochronology

Clay minerals in sample 3404325 form mottled domains where boundaries of individual flakes are difficult to distinguish (Supplementary Fig. S2). Illite grains preserve their primary compaction structures, wrapping around detrital, angular quartz grains (dashed lines in Supplementary Figure S2). In contrast, clays in samples 3404236 are large and angular. Illite grains in this sample show discrete, sharp grain boundaries (solid white lines in Supplementary Fig. S2). Of the two siltstone/shale samples analysed for Rb–Sr geochronology, 3404236 (upper Sturt Formation) and 3404235 (lower Sturt Formation), only the latter sample yielded a meaningful result. The analyses on sample 3404236, $n = 60$, had little spread in Rb/Sr ratios and a low percentage of radiogenic Sr ($^{87}\text{Sr}/^{86}\text{Sr} < 0.8$); nonetheless, a date of 839 ± 235 Ma was obtained with an initial $^{87}\text{Sr}/^{86}\text{Sr}$ of 0.7030 ± 0.0127 (Fig. 8). For sample 3404235, $n = 51$, there was

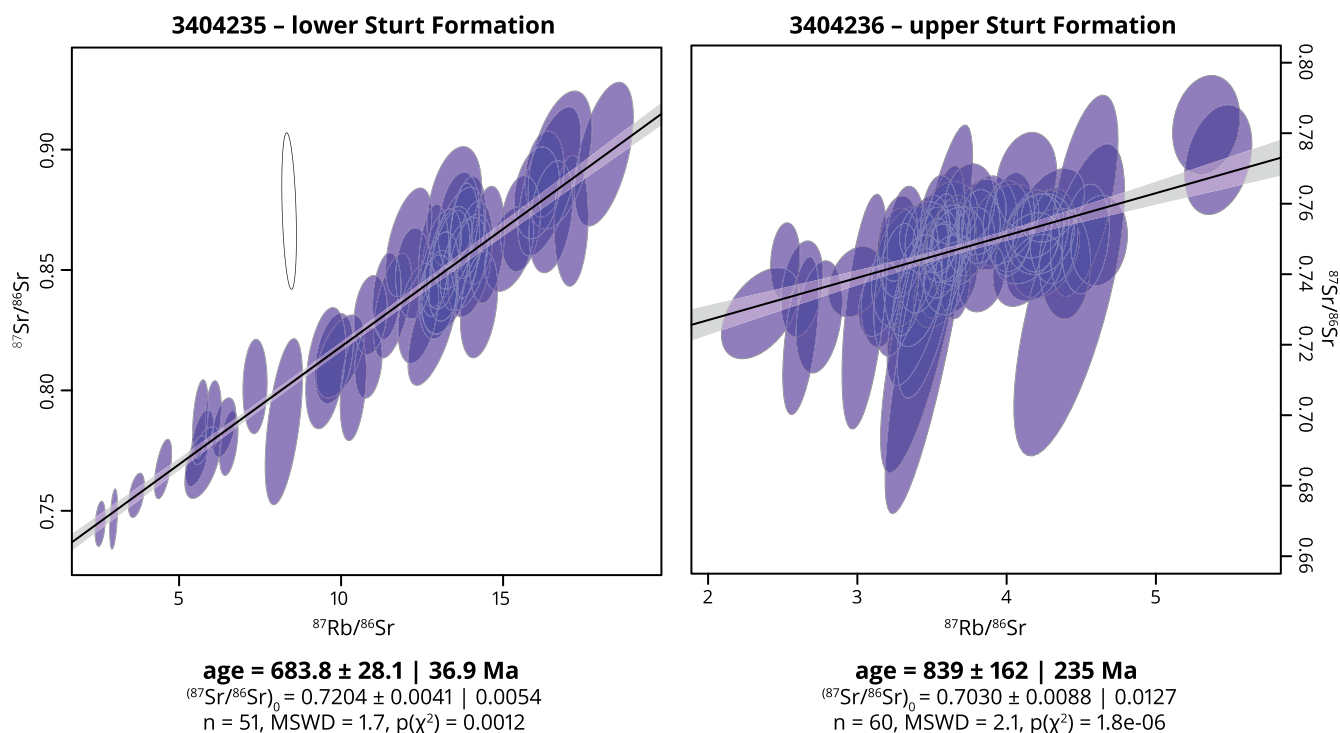


Figure 8. (Colour online) Rb–Sr isochrons of the two shale/siltstone samples from the Sturt Formation in drillhole SR13/2 analysed in this study. Quoted uncertainty and ellipses are two standard errors (2SEs). The second uncertainty term accounts for overdispersion. Generated using IsoplotR (Vermeesch, 2018), without the decay constant uncertainty propagated. ^{87}Rb decay constant used = $(1.3972 \pm 0.0045) \times 10^{-11} \text{ a}^{-1}$.

reasonable spread in Rb/Sr ratios and a date of $684 \pm 37 \text{ Ma}$ with an initial $^{87}\text{Sr}/^{86}\text{Sr}$ of 0.7204 ± 0.0054 was obtained (Fig. 8).

5. Discussion

5.a. Zircon trace element geochemistry

Zircons analysed in this study mostly show affinity to generation in continental crust with only a small number of zircons potentially of oceanic affinity (Supplementary Fig. S3), as inferred by the U/Yb against Y plot (Grimes *et al.* 2007, 2015). Almost all zircons have a Th/U ratio >0.07 and are inferred to be magmatic rather than metamorphic as Th preferentially partitions into common metamorphic minerals, e.g. monazite and allanite (Rubatto, 2002; Collins *et al.* 2004). C1 chondrite normalized (O'Neill, 2016) lanthanoid concentrations are generally typical for zircon (Supplementary Fig. S1) with a positive slope (increasingly negative λ_1 values) from light to heavy lanthanoids, a positive Ce anomaly and negative Eu anomaly (Hoskin & Ireland, 2000; Hoskin & Schaltegger, 2003). There is no apparent trend in lanthanoid slope or curvature (Supplementary Fig. S4), denoted as λ_1 (linear slope), λ_2 (quadratic slope) and λ_3 (cubic slope) (Anenburg, 2020), with time or sample. Both Eu and Ce anomalies (denoted by Eu^* and Ce^*) show a scattered distribution through time (Supplementary Fig. S4). The youngest few zircons c. 670 Ma, although limited in number, have out-of-phase Eu^* (low) and Ce^* (high) anomalies suggestive of growth in competition with plagioclase and not reflective of magma oxidation state (Verdel *et al.* 2021).

5.b. Provenance and MDAs

5.b.1. Maximum depositional ages

The older limit of expected depositional age for samples in this study is constrained by two DZ MDAs from the underlying Belair

Subgroup, namely the Gilbert Range Quartzite ($731 \pm 34 \text{ Ma}$, Keeman *et al.* 2020; Lloyd *et al.* 2020) and Mitcham Quartzite ($720 \pm 21 \text{ Ma}$, van der Wolff, 2020). The younger age limit for deposition of the Yudnamutana Subgroup is constrained by a $663.03 \pm 0.76 \text{ Ma}$ tuff in the Wilyerpa Formation (Cox *et al.* 2018). The Serle Conglomerate is older than the c. 642 Ma minimum depositional age of the Tapley Hill Shale (Re–Os shale, Kendall *et al.* 2006) that it is interpreted to underlie.

An MDA of $1134 \pm 24 \text{ Ma}$ was obtained for the combined Fitton Formation samples. This is significantly older than the expected depositional age c. 730–663 Ma.

The MDAs for the Sturt Formation, both existing and newly obtained, are presented in Table 1 according to the groupings outlined in section 4.a.2 above. There is significant scatter in MDAs across samples from the Sturt Formation; however, DZ age spectra are similar (Figs. 7, 9) throughout all samples (spanning more than 500 km north–south, Fig. 1). Three independent samples covering a distance of ~250 km north–south have MDAs within uncertainty of each other. While DZ population spectra variations occur locally, as is expected across a large basin, and with significant recycling of underlying stratigraphy in glacially derived sediment, the remarkable similarity of most samples' spectra (Figs. 7, 9) is consistent with lithostratigraphic mapping, which indicates that these units are correlative. In addition, many researchers have noted that the Sturt Formation often consists of two diamictite-abundant units separated by an argillaceous or arenaceous sequence (Lechte & Wallace, 2015; Virgo *et al.* 2021). Different regions of the basin likely preserve deposits from different parts of the Sturtian glacial event where the two diamictite-abundant units may represent discrete periods of glacial advance or various phases of the glaciation (Lechte & Wallace, 2015; Lechte *et al.* 2018). Chronological constraints for the Sturt Formation had been almost non-existent up until recently but are now robust enough to

Table 1. Sturt Formation MDAs

Location	Existing MDA*	New MDA
South Mount Lofty Ranges (Sturt Gorge, Adelaide)	714 ± 28 Ma	1007 ± 14 Ma
North Mount Lofty Ranges (Clare Valley)		1743 ± 34 Ma
South Flinders Ranges (Pichi Richi Pass):	667 ± 6 Ma	
North Flinders Ranges (Copley area)		663 ± 11 Ma, 698 ± 12 Ma
North Flinders Ranges (Yankaninna area)		1185 ± 23 Ma
North Flinders Ranges (Vulkathuhna-Gammon Ranges)		891 ± 15 Ma
North Flinders Ranges (Stubbs Waterhole, Arkaroola)		1178 ± 20 Ma
North Flinders Ranges (Stanley Mine, Arkaroola)		1096 ± 22 Ma
North Flinders Ranges (Willouran Ranges)	673 ± 19 Ma	

*Keeman *et al.* (2020); Lloyd *et al.* (2020).

bracket deposition of the Sturt Formation and Fitton Formation to between 720 ± 21 Ma and 663.03 ± 0.76 Ma (Fanning & Link, 2008; Cox *et al.* 2018b; Keeman *et al.* 2020; van der Wolff, 2020). Given the younger limit imposed by the Wilyerpa Formation tuff, the MDA of c. 663 ± 11 Ma is likely close to the true depositional age for at least the terminal deposits (upper portion) of the Sturt Formation.

GSNSWKB002 was a reconnaissance sample collected from undifferentiated Yancowinna Subgroup in the Barrier Ranges of New South Wales to test the general correlation with the Yudnamutana Subgroup of South Australia. This area is the easternmost known extension of the Adelaide Superbasin during the Neoproterozoic (Cooper & Tuckwell, 1971; Cooper, 1973; Preiss, 1987; Fitzherbert & Downes, 2015; Lloyd *et al.* 2020). The sample is from a highly weathered diamictite with clasts ranging up to pebble size and a silty to fine sand matrix. An MDA of 1065 ± 18 Ma was obtained from the sample, with a DZ population spectrum similar to that of the probable correlatives in South Australia (Figs. 7, 9). This provides limited but supporting evidence of a shared detrital source and that these two subgroups are correlative as is indicated by the existing lithostratigraphic framework (Lloyd *et al.* 2020).

An MDA of 1477 ± 33 Ma was obtained from the Wilyerpa Formation (FR1_005_02) sampled in the Clare Valley. This is significantly older than the expected depositional age (i.e. c. 663 Ma) and may be a factor of low zircon yield and/or no zircon close to depositional age being present in the sample.

An MDA of 1246 ± 24 Ma was obtained from the Serle Conglomerate sample (FR3_004). Again, this is significantly older than true depositional age, which is expected to be between c. 663 Ma and c. 642 Ma. The DZ population spectrum somewhat differs (Figs. 7, 9) from the nearby Sturt Formation sample (FR3_006), although this may partially be an artefact of the much lower zircon yield from the Serle Conglomerate sample.

5.b.2. Provenance

Two DZ populations, c. 1840–1790 Ma and c. 1640–1580 Ma, form major peaks in virtually all samples. The exact age positions and magnitude of the population peaks vary slightly by sample, with broad north–south and east–west variations, generally trending to older Palaeoproterozoic age populations in the west and south. It is likely that there is significant recycling of the unconformably underlying stratigraphy due to sub-glacial erosion (Young &

Gostin, 1989b). The similarity of the DZ spectra within the samples of this study to each other, and to earlier rocks of the Adelaide Superbasin (Fig. 9), suggests homogenization of detrital material over a large area, potentially with extra-basin material, as well as intra-basin recycling of earlier stratigraphy, presumably by glacial erosion.

Zircons with ages greater than c. 1400 Ma are likely sourced locally from the Gawler Craton, Barossa Complex and Curnamona Province that collectively record numerous zircon generation events and sedimentary sequences known to contain DZ of these ages (Swain *et al.* 2005; Fanning *et al.* 2007; Barovich & Hand, 2008; Conon & Preiss, 2008; Reid *et al.* 2008; Stevens *et al.* 2008; Belousova *et al.* 2009; Fraser & Neumann, 2010; Fraser *et al.* 2010; Jagodzinski & Fricke, 2010; Wade, 2011; McAvaney, 2012; Meaney, 2012; Reid & Hand, 2012; Kromkhun *et al.* 2013; Morrissey *et al.* 2013; Reid *et al.* 2014a; Reid *et al.* 2014b; Jagodzinski & McAvaney, 2017; Meaney, 2017; Reid & Payne, 2017; Reid *et al.* 2017; Morrissey *et al.* 2018; Morrissey *et al.* 2019; Reid, Halpin & Dutch, 2019; Jagodzinski *et al.* 2020; Reid *et al.* 2021). The southernmost samples from Sturt Gorge are dominated by c. 1840 Ma zircons, and northward progression through the basin system generally sees a shift in dominance of the c. 1840 Ma population to the younger c. 1590 Ma population of zircon. This observation is likely a result of the variation in local basement geology of the Gawler Craton and Curnamona Province near the sample sites.

The generally minor Stenian population of zircon at c. 1160 Ma suggests provenance from the Musgrave Province (Smithies *et al.* 2008; Wade *et al.* 2008; Smithies *et al.* 2011; Smits *et al.* 2014), but as noted in Lloyd *et al.* (2022), they may be sourced from an as yet undiscovered but inferred late Mesoproterozoic (c. 1300–1000 Ma) source to the east (Wyszczanski & Allibone, 2004; Fergusson *et al.* 2007; Mackay, 2011; Korsch *et al.* 2012). This Stenian zircon population is generally more abundant in samples closer to the eastern and western margins of the basin (Figs. 7, 1). Alternative sources of this late Mesoproterozoic zircon could be the South Tasman Rise (Fioretti *et al.* 2005), Coompana Province (Pawley *et al.* 2020) or far-field transport across Antarctica from the Tonian Oceanic Arc Super Terrane (Jacobs *et al.* 2015). Again, recycling of underlying stratigraphy is a likely source of some of these zircons.

Neoproterozoic zircons with ages between c. 900 Ma and c. 780 Ma can be attributed to igneous events early in the Adelaide Superbasin. The known igneous events of the Adelaide Superbasin

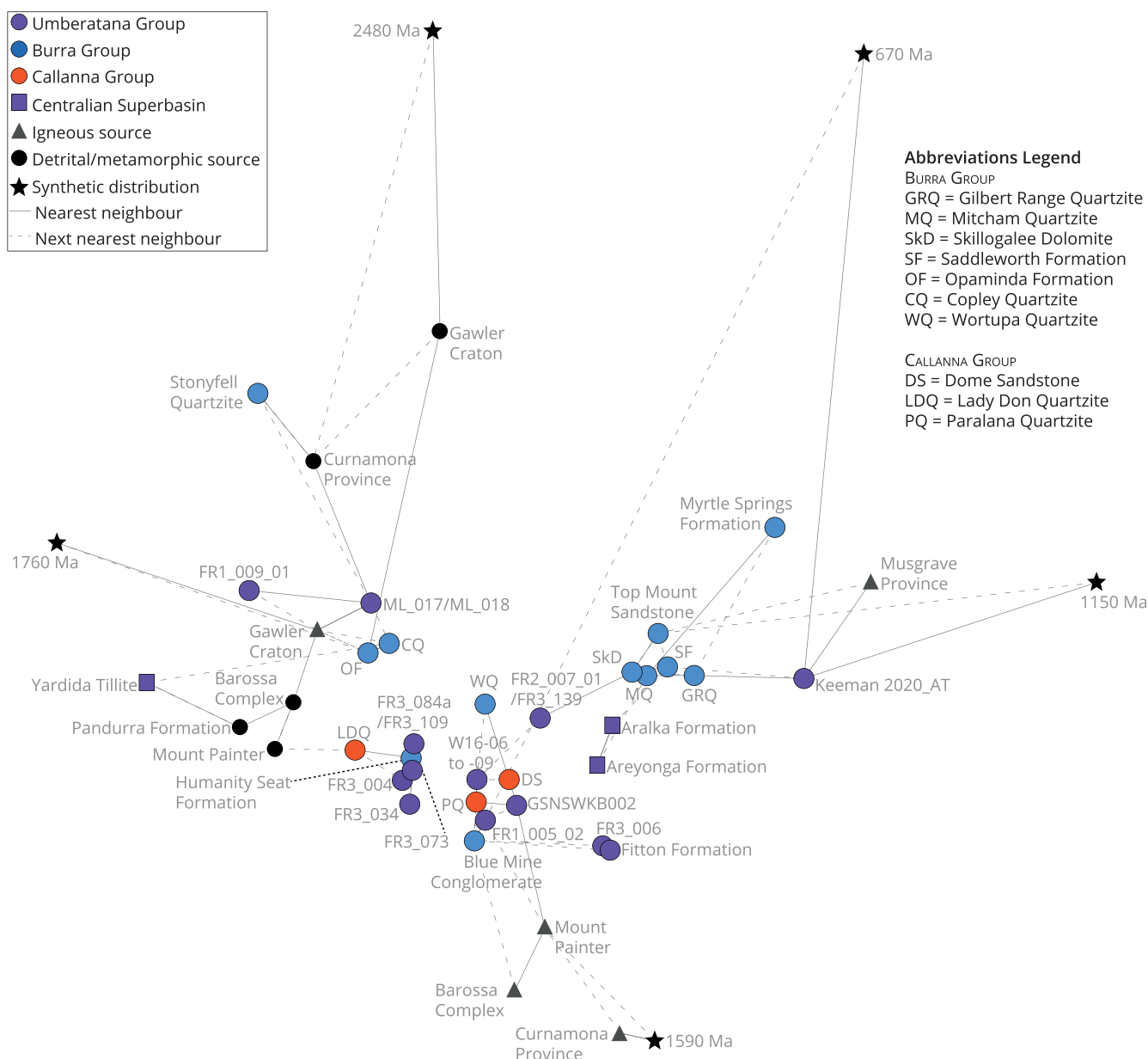


Figure 9. (Colour online) Non-metric multidimensional scaling plot of samples analysed ($n > 30$) in this study (purple circles) with data from potential correlative formations of the Centralian Superbasin (purple squares), potential source regions (black and grey circles and triangles), older stratigraphy within the basin (blue and orange circles) and synthetic distributions (black stars) generated from the primary and secondary peaks of a KDE that combines all new data in this study. This plot shows relative similarity of all data to each other and is intended as a visual guide. Points that plot closer together suggest greater similarity and points that plot further away from each other indicate greater dissimilarity. Axes are omitted as the algorithm used produces normalized values with no physical meaning and can be safely removed. Produced using IsoplotR with the Kolmogorov-Smirnov metric (Vermeesch, 2018).

for this time period are the Willouran Large Igneous Province c. 830 Ma (Wingate *et al.* 1998; Preiss, 2000; Wade *et al.* 2014; Lloyd *et al.* 2022), Oodla Wirra Volcanics c. 798 Ma (Fabris *et al.* 2005), Boucaut Volcanics c. 788 Ma (Armistead *et al.* 2020) and magmatism associated with the Koorunga Member of the Skillogalee Dolomite c. 70 Ma (Preiss *et al.* 2009).

Zircon younger than 780 Ma is much more difficult to reconcile. It is apparent that some zircon-bearing igneous events were occurring c. 700 Ma to c. 660 Ma, and that these zircons were in the sediment supply of the Sturt Formation. The igneous events may have been distal to the basin and may have occurred as short-lived pulses. While a 663.03 ± 0.76 Ma tuff has been dated (Cox

et al. 2018b) from within the Wilyerpa Formation immediately post-dating deposition of the Sturt Formation, the site of the volcanic centre for the ashfall is unknown. Additionally, zircon of c. 700–660 Ma within the Sturt Formation has so far only been found on the far western margin of the Adelaide Rift Complex within the Adelaide Superbasin (Fig. 10), indicating this magmatic source may have been to the west of or on the western margin of the basin.

Within the Centralian Superbasin, the syn-glacial Yardida Tillite and Areyonga Formation, and the post-glacial Aralka Formation are suggested as correlatives of the Sturt Formation and Tapley Hill Formation, respectively (Preiss *et al.* 1978;

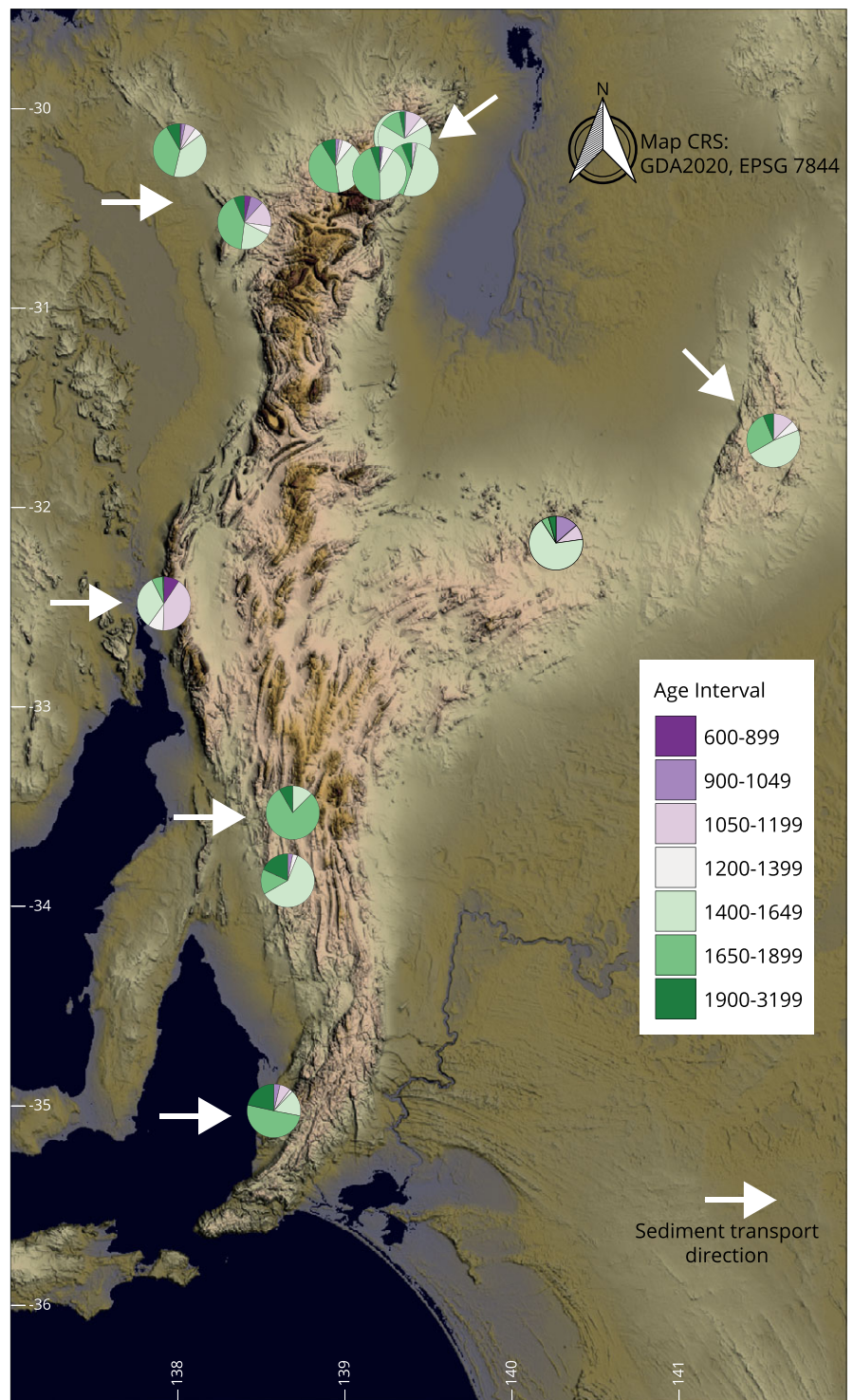


Figure 10. (Colour online) Schematic map with pie charts at sample locations to highlight the changes in zircon population spectra relative to geographic location. Arrows are generalized schematic indicators of palaeo-sediment transport direction. Includes data from this study, Preiss (2014), Keeman *et al.* (2020) and Lloyd *et al.* (2020).

Edgoose, 2013; Kruse *et al.* 2013; Normington & Donnellan, 2020). Interestingly, the DZ age spectrum of the Yardida Tillite (Georgina Basin, Northern Territory/Queensland) is very similar (Fig. 9) to that of the local basement of South Australia (e.g. Gawler Craton). This is explained by its proximity to the Mount Isa and Aileron provinces, suggested to be the primary zircon source for the Yardida Tillite (Verdel *et al.* 2021). These provinces host abundant c. 1850–1640 Ma zircon that is also found in the Gawler Craton and Curnamona Province. In addition,

palaeomagnetic and geological reconstructions for the time suggest that the South Australian Craton may have been rotated closer to the Georgina Basin at that time (Li & Evans, 2010; Lloyd *et al.* 2020). The DZ age spectra of the Areyonga Formation and Aralka Formation (Amadeus Basin, Northern Territory/Western Australia) are similar to the Burra Group and Sturt Formation samples (Fig. 9) from the western margin of the Adelaide Rift Complex. All these units may have received zircons from the Musgrave Province where Stenian-aged zircons are abundant,

and both basins have abundant nearby sources of pre-Stenian zircon. Notably, no zircon younger than c. 800 Ma has been found in the Areyonga and Aralka formations to date.

5.b.3. Comparison to palaeocurrent data

Observations drawn in this study from DZ generally support existing palaeocurrent data. Palaeocurrent data from the Yudnamutana Subgroup suggest a westerly transport direction in the Mount Painter area and along the Paralana fault system, northerly transport on the northern side of the Gammon syncline and Yankaninna anticline and north-easterly transport along the western edge of the Adelaide Rift Complex (Copley area, south-eastern Willouran Ranges) (Link & Gostin, 1981; Young & Gostin, 1989b; Young & Gostin, 1991). It is likely that underlying strata were recycled by sub-glacial erosion, making the use of DZ spectra for determining palaeo-transport paths difficult. However, the only area where detrital data from this study potentially differ in transport direction from the existing palaeocurrent data is the Vulkathuhna-Gammon Ranges. The DZ populations in our data (Fig. 7: FR3_073, Fitton Formation samples) are most similar (Fig. 9) to older stratigraphy of the basin and to nearby basement sources located to the northeast (Fig. 1). This suggests a south or south-westerly sediment transport (Fig. 10) direction from these neighbouring basement sources into the depocentre.

5.c. Rb–Sr geochronology

In-situ Rb–Sr geochronology is a rapidly developing technique that, when applied to shales, can provide information about depositional ages or early diagenetic illite formation (Subarkah *et al.* 2021). In shales, the Rb–Sr isotopic system is susceptible to low–moderate temperature hydrothermal alteration and can be influenced by detrital input (Subarkah *et al.* 2022) meaning that careful assessment must be done before assigning geological significance to obtained isochron ages. For the two samples analysed in this study, the obtained dates must be between 730 Ma and 663 Ma for them to be representative of depositional age. Uncertainties quoted in this section include propagation of the decay constant uncertainty on ^{87}Rb (~0.32%, Villa *et al.* 2015) to enable comparison to other geochronometric systems (e.g. U–Pb).

The 839 ± 241 Ma date obtained for sample 3404236 (Fig. 8) is not a meaningful date due to large uncertainty, and the old isochron date suggests it contains a significant detrital component. The clay morphologies of the sample (Supplementary Fig. S2) are large and sub-rounded, with distinct edges and preserving their internal structure. These morphologies are characteristic of detrital illite (Rafiei & Kennedy, 2019; Deepak *et al.* 2022) and have been identified elsewhere in the late Neoproterozoic sections of the Adelaide Superbasin (Rafiei *et al.* 2020). These concerns also apply to former attempts to date the overlying Tapley Hill Formation via traditional whole rock Rb–Sr methods (Webb, 1980; Webb *et al.* 1983). The 684 ± 37 Ma (Fig. 8) date obtained for sample 3404235 is consistent with the constrained depositional age for the Sturt Formation and can be considered a meaningful, syn-depositional age. The clay minerals in this sample appear to have formed within the sediment (Supplementary Fig. S2), where illite appears moss-like, fills pore spaces and wraps around detrital grains.

5.d. Tectonic and palaeogeographic implications

While the DZ and palaeocurrent datasets need to be expanded in future to cover more of the basin, particularly to the east (Olary area, and New South Wales) and far northwest (Davenport and

Denison Ranges), some inferences can be made regarding the palaeogeography and tectonics of the Adelaide Superbasin during the Cryogenian. Firstly, it is apparent that the DZ spectrum of each sample is highly dependent on local geology, commonly recycling the underlying stratigraphy and/or derived from the nearby basement geology. Recycling of underlying material supports the common observation that clasts in diamictite of the Yudnamutana Subgroup can be identified as derived from the Burra Group and, locally, the Callanna Group (Coats & Preiss, 1987). During deposition of the preceding Burra Group, far-field sediment supply dominated; however, locally derived detritus became much more prominent during the deposition of the Yudnamutana Subgroup implying a change in the mechanism of sediment transport (e.g. glacial ice).

Secondly, active zircon-bearing magmatism occurred at c. 700–660 Ma, although the location and volume of this magmatism remain unknown. The spatial distribution of the samples containing Cryogenian zircon (Fig. 10) suggests that the source was to the west, or along the western margin, of the basin. Of note, there is a conglomerate with basalt clasts at the top of the Sturt Formation at the central-western margin (Depot Creek) of the Adelaide Rift Complex (Hopton, 1983), however, its origin and age remain enigmatic.

Thirdly, the DZ spectrum of the Yancowinna Subgroup sample supports a common sediment source with the Sturt Formation samples in the northeast of the basin, consistent with earlier palaeogeographic interpretations that the Curnamona Province was a topographic high between these two regions and was shedding detrital material to both. The data presented here also support the Yancowinna Subgroup being correlative to the Yudnamutana Subgroup, as suggested by the current stratigraphic framework (Cooper & Tuckwell, 1971; Cooper, 1973; Preiss, 1987; Fitzherbert & Downes, 2015; Lloyd *et al.* 2020).

In combination with glacial scouring, it is clear that active tectonics played a significant control on the dramatic thickness variations of the Yudnamutana Subgroup sedimentary rocks (Young & Gostin, 1991; Preiss *et al.* 2011; Le Heron, 2012; Le Heron *et al.* 2014). The Yudnamutana, Baratta and Torrowangee troughs (Fig. 1) are major extensional sub-basins bounded by mappable normal growth faults (Preiss, 1985; Preiss & Conor, 2001; Preiss *et al.* 2011). This normal faulting has been interpreted to record the final phase of rifting associated with continental separation (Preiss, 2000), although Merdith *et al.* (2017) considered that the rift-drift transition of the Australia–Laurentia margin occurred earlier at c. 780 Ma. While the debate regarding timing of rift–drift transition is beyond the scope of this research, it is unlikely to be resolved in the northern regions of the basin given it is distal to the margin of the palaeo-Pacific Ocean. Contrastingly, near the basin margin proximal to the inferred location of the palaeo-Pacific (southern and eastern regions), a change in the rate of accommodation space creation should be evident. This rate change in accommodation space creation would coincide with the rift-drift transition as active rifting is expected to stop once ocean-crust formation is underway.

5.e. Sturtian nomenclature

5.e.1. South Australian formal stratigraphy

The correlation of diamictite-abundant units of the Yudnamutana Subgroup was subject to much debate during the 1970s and 1980s, with arguments both for and against these rocks representing two discrete glacial events separated by an

unconformity (Coats & Forbes, 1977; Murrell *et al.* 1977; Coats & Preiss, 1987). Subsequent research showed that the rocks named ‘Tillites’ of the Yudnamutana Subgroup were consistent with only one glacial event (Preiss, 1993; Preiss *et al.* 1998; Preiss, 2000) but representing ice sheet advance-retreat cycles (Le Heron, 2012). The conjecture regarding correlation of the diamictite-abundant units using a specific clast type, and mapping by numerous individuals over a long period of time, has led to six formal names for a unit that is now known to be correlative across the entire Adelaide Superbasin. The six different names for what are the same unit have led to unnecessary artefacts on geologic maps (e.g. a unit changing name across a map sheet boundary) and can be confusing to those who are unfamiliar with local formal stratigraphic nomenclature.

No significant lithological differentiation distinguishes the diamictite-abundant units (Fig. 5) within the Yudnamutana Subgroup from each other, and both stratigraphic position and geochronology support their broad equivalence (Young & Gostin, 1989b; Preiss *et al.* 1998, 2011; Cox *et al.* 2018b; Keeman *et al.* 2020; Lloyd *et al.* 2020; this study). Considering this evidence, we propose a refined stratigraphic nomenclature for the diamictite-abundant formations of the Yudnamutana Subgroup (e.g. Appila Tillite, Bolla Bollana Tillite, Sturt Tillite) as the Sturt Formation (Fig. 3). The name ‘Sturt’ is retained as the first glacial diamictite formally named the Sturtian tillite (Howchin, 1920; Mawson & Sprigg, 1950); therefore, it takes precedence over all other correlative formation names. Furthermore, it has become eponymous with the global Sturtian Glaciation. ‘Tillite’ has been dropped in favour of ‘Formation’ as, while glacial diamictite is the most distinctive lithology, it was not exclusively deposited by the direct action of glacial ice (much of it is glaciomarine) and is not the most volumetrically abundant rock type within the Sturt Formation across the entire Adelaide Superbasin (Preiss *et al.* 2011). Instead, the Sturt Formation comprises numerous lithologies that were deposited under general glacial conditions (Link, 1977; Link & Gostin, 1981; Preiss, 1987; Preiss, 2000; Preiss *et al.* 2011; Virgo *et al.* 2021). The use of ‘Formation’ instead of ‘Tillite’ was proposed previously by Murrell *et al.* (1977) and follows the international stratigraphic guide. A formal definition card accompanies this paper as Appendix 2, with the generalized stratigraphic logs of the type and reference sections presented in Figures 4 and 5. An additional stratigraphic log from drillhole SR13/2 on the Stuart Shelf is provided in Supplementary Figure S4.

5.e.2. Sturtian Glaciation (Cryochron)/Laurentian Neoproterozoic Glacial Interval

Le Heron *et al.* (2020) proposed that the name ‘Laurentian Neoproterozoic Glacial Interval’ be used in favour of the name ‘Sturtian Glaciation’ for the first of two, major pan-glacial events recognized in Cryogenian rocks. Further, they suggest that the term ‘Sturtian Glaciation’ should be exclusively used for Australian strata, and that the global geochronologic data permit only a short 2.4 Ma long global glacial event or diachronous shifting of ice-centres across Rodinia. While Le Heron *et al.* (2020) highlight the issue of interpreting results in a model-led approach, a notion we agree on, we disagree with their suggestion that use of the name Sturtian Glaciation for the first major Cryogenian pan-glacial event is no longer justifiable. This suggestion was primarily based on their interpretation that most rocks representing the Sturtian Glaciation in Australia chronometrically lie outside of the Sturtian glacial interval, c. 717–661 Ma (Rooney *et al.* 2015; Rooney *et al.* 2020). Only the tuff from near the base of the Wilyerpa Formation

(663.03 ± 0.76 Ma, Cox *et al.* 2018b) was considered to be within the time interval defined for the Sturtian glacial event; this argument was reiterated by Kennedy *et al.* (2020).

However, the interpretation by Le Heron *et al.* (2020) appears to hinge on the previous lack of data from early Cryogenian glacial (Yudnamutana Subgroup) and late Tonian pre-glacial (Burra Group) sequences in South Australia. Even with the challenges associated with constraining deposition by DZ studies, two studies (Keeman *et al.* 2020; Lloyd *et al.* 2020) have provided MDA constraints from the Sturt Formation (Table 1). This study presents a further ten DZ samples with two samples yielding MDAs within the 717–661 Ma period (Table 1), and a new in-situ Rb–Sr age from the Sturt Formation of 684 ± 37 Ma (Fig. 8). Importantly, DZ MDA constraints from the underlying Belair Subgroup (Fig. 2), namely the Gilbert Range Quartzite (731 ± 34 Ma, Keeman *et al.* 2020; Lloyd *et al.* 2020) and Mitcham Quartzite (720 ± 21 Ma, van der Wolff, 2020), provide maximum age estimations for when final deposition of the upper Burra Group began.

Additionally, Le Heron *et al.* (2020) consider the Cox *et al.* (2018b) tuff age (Wilyerpa Formation, AUS) to be an MDA; however, both Fanning and Link (2006) and Cox *et al.* (2018b) demonstrate that the tuff is syn-depositional, with their dating indicating volcanism was coeval with deglaciation. The tuff age provides neither a maximum nor minimum age for the Wilyerpa Formation as it occurs ~80 m below the base of the Tapley Hill Formation; however, it provides a robust minimum age constraint for the underlying Sturt Formation.

Thus, the MDAs from the underlying Burra Group and the syn-depositional tuff in the Wilyerpa Formation require that rocks representing the early Cryogenian Sturtian Glaciation in South Australia (Sturt Formation, Fitton Formation) were deposited ≤730 Ma and ≥663 ± 0.76 Ma, thereby independently constraining the age of the Sturt Formation to the globally defined interval for the Sturtian Glaciation (Rooney *et al.* 2015; Rooney *et al.* 2020). Initiation of final deglaciation for the Sturtian Glaciation can also be constrained, albeit loosely, by data in this study to c. 674–663 Ma, as sample FR3_139 from the upper Sturt Formation (MDA: 663 ± 11 Ma) came from the same stratigraphic interval as the Wilyerpa Formation tuff.

Furthermore, data from our study refute the Le Heron *et al.* (2020) suggestion of a short, 2.4 million year, Sturtian Glaciation, 659.6 ± 10.2 Ma to 657.2 ± 5.4 Ma, based on Re–Os ages from the Aralka Formation (Kendall *et al.* 2006), and Ballachulish Slate (Rooney *et al.* 2011) as the Australian Sturtian Glaciation deposits are definitively older than this proposed interval, there is an erosional unconformity between the Yudnamutana Subgroup rocks and the overlying post-glacial transgressive sequences, and the Aralka Formation is demonstrably post-glacial.

In contrast to the Wilyerpa Formation tuff, Le Heron *et al.* (2020) interpret the age of an epiclastic tuff in the Pocatello Formation, USA (Fanning & Link, 2004), as a minimum age estimate for the formation. This epiclastic tuff from the upper diamictite of the Pocatello Formation has been re-evaluated as an MDA and may actually be from a late Cryogenian Marinoan glacial sequence, unconformably overlying a non-glacial sequence, which in turn unconformably overlies a lower Sturtian glacial sequence (Isakson, 2017). Additionally, Isakson (2017) had earlier revised several of the igneous ages presented in the Le Heron *et al.* (2020) compilation, notably a syn-Sturtian age of the Hogback Rhyolite from 684 ± 4 Ma (Lund *et al.* 2003; Lund *et al.* 2010) to

693.03 ± 0.73 Ma. Isakson (2017) presented two additional ages, 697.05 ± 0.28 Ma and 697.78 ± 0.18 Ma, from volcanics in the lower Scout Mountain Member of the Pocatello Formation, previously interpreted to be 686 ± 4 Ma (Fanning & Link, 2008). The data of Keeley *et al.* (2013) from the lower Scout Mountain member (685 ± 0.4 Ma) are presented as a depositional age by Le Heron *et al.* (2020), rather than as an MDA as the original authors and Isakson (2017) present.

Available geochronology suggests that deposition of early Cryogenian glaciogenic rocks in at least Australia (Keeman *et al.* 2020; Lloyd *et al.* 2020; this study), Arabia/Nubia (MacLennan *et al.* 2018; Park *et al.* 2019), Baltica (Środoń *et al.* 2022), Laurentia (Rooney *et al.* 2014; Isakson, 2017; Macdonald *et al.* 2018), South China (Song *et al.* 2017; Wang *et al.* 2019; Lan *et al.* 2020; Rooney *et al.* 2020) and Siberia (Rud'ko *et al.* 2020) occurred globally within the c. 717–661 Ma interval. These ages cannot eliminate some diachroneity in the timing of onset of glaciation or the possibility of glacial advance and retreat cycles. Globally, final deglaciation appears to be relatively synchronous at c. 663–661 Ma (Fig. 6).

While Figure 6 and the equivalent diagram in Le Heron *et al.* (2020) provide brevity for visualization and assessment of the expanding global Cryogenian geochronologic datasets, they lack detailed stratigraphic context and methodology: unavoidable limitations for this style of diagram, with size, legibility and accessibility considerations all contributing factors (e.g. Cramer *et al.* 2020). The ideal, more accurate representation of global Cryogenian chronostratigraphic datasets would include detailed stratigraphic logs, accompanying regional correlations, and detailed geochronometric methodology and results. In some regions, these datasets are currently unavailable, unreliable or limited.

The apparent diachroneity of glacial onset present in Laurentia (Fig. 6) is likely a result of complexity in zircon age determinations and chronostratigraphic misinterpretations (e.g. syn-depositional instead of MDA). Eyster *et al.* (2018) also highlight how this style of misinterpretation was used to argue for diachroneity of onset (Baldwin *et al.* 2016). Careful scrutiny of geochronologic data, its methodological limitations and its chronostratigraphic interpretation is essential to prevent spurious conclusions.

6. Conclusions

This research provides an updated chronostratigraphic framework for the Yudnamutana Subgroup of South Australia and presents it in the context of global Cryogenian chronostratigraphic data and their interpretations. Additionally, the lithostratigraphy representing the main diamictite-abundant units of the Yudnamutana Subgroup (Appila Tillite, Bolla Bollana Tillite, Calthorinna Tillite, Merinjina Tillite, Pualco Tillite and Sturt Tillite) is consolidated and redefined as the Sturt Formation based on their lithostratigraphic similarity and stratigraphic position, with support from DZ age spectra. Furthermore, DZ age spectra support lithostratigraphic correlation of Yancowinna Subgroup (New South Wales) with the Yudnamutana Subgroup (South Australia).

The Sturt Formation was deposited $\leq 720 \pm 21$ Ma (van der Wolff, 2020), and prior to 663.03 ± 0.76 Ma (Cox *et al.* 2018b), with the upper part of the unit being deposited c. 673–663 Ma, providing further support to prior studies (Keeman *et al.* 2020; Lloyd *et al.* 2020). In-situ Rb–Sr dating of the lower Sturt Formation yielded an age of 684 ± 37 Ma that is interpreted to be a syn-depositional age. Broadly equivalent DZ age spectra (Fig. 9) for

samples from the Sturt Formation (with local variation) and similarity to underlying Burra and Callanna Group rocks suggest recycling of underlying stratigraphy and sourcing of detritus from local basement rocks consistent with the common occurrence of clasts derived from the underlying geology.

Here we refute the suggestion of a short (2.4 Ma) global glacial event (Le Heron *et al.* 2020), which is based on their interpretation that most stratigraphy (with the exception of the Wilyerpa Formation tuff) representing the Sturtian Glaciation in South Australia lies chronometrically outside the defined global interval (717–661 Ma). The data in this and prior (Keeman *et al.* 2020; Lloyd *et al.* 2020) studies from the Sturt Formation fall within the globally defined Sturtian event (Rooney *et al.* 2015), and we demonstrate how the data interpreted by Le Heron *et al.* (2020) can be reinterpreted to also support this duration for the Laurentian early Cryogenian glaciations (Keeley *et al.* 2013; Isakson, 2017). Additionally, we provide an updated compilation of global geochronology data for the Cryogenian (Fig. 6), which shows relatively synchronous deglaciation globally for the Sturtian Glaciation, while showing some diachroneity for onset with the caveat that this figure can be misinterpreted. Our study supports the continued use of Sturtian Glaciation or *cryochron* globally for the first major pan-glacial event recorded in Cryogenian stratigraphy and does not support using Laurentian Neoproterozoic Glacial Interval in its place.

Supplementary material. The supplementary material for this article can be found at <https://doi.org/10.1017/S0016756823000390>

Data availability statement. Complete data for this publication are freely available for download from figshare at the following links. These datasets contain all the U–Pb geochronology data, trace element data, Rb–Sr geochronology data and basic sample metadata. Supplementary figures and appendices are available from the Cambridge Journals Online website.

Zircon and NIST standards data for all analytical sessions: <https://doi.org/10.6084/m9.figshare.18131432>

Yudnamutana Subgroup detrital zircon data (this study): <https://doi.org/10.6084/m9.figshare.19181144>

Zircon CL images: <https://doi.org/10.6084/m9.figshare.19181024>

Shale Rb–Sr data: <https://doi.org/10.6084/m9.figshare.21624162>

Acknowledgements. We acknowledge the Adnyamathanha, Arabana, Bangarla, Kurna, Kokatha, Ngadjuri and Nukunu Peoples as the traditional owners and custodians of the land on which this research was conducted. We acknowledge and respect their deep feelings of attachment and spiritual relationship to Country, and that their cultural and heritage beliefs are still as important to the living people today.

The authors acknowledge the instruments and scientific and technical assistance of Microscopy Australia at Adelaide Microscopy, The University of Adelaide, a facility that is funded by the University, and State and Federal Governments. Particular thanks to Aoife McFadden for their assistance with SEM-CL imaging.

We also thank James Nankivell (University of Adelaide) for their assistance with fieldwork, and the Geological Survey of South Australia and MinEx CRC for funding the research. Chris Folkes (Geological Survey of New South Wales) and John Greenfield (formerly GSNW) are thanked for their expertise on the New South Wales sequences. Arkaroola Wilderness Sanctuary and Operation Flinders (Yankaninna Station) are thanked for their generous hospitality during fieldwork on their properties.

We would also like to thank Galen Halverson, Nick Christie-Blick and two anonymous reviewers for their constructive comments that greatly improved this manuscript.

This work was conducted with the relevant permissions and scientific permits from the relevant stakeholders. This publication forms MinEx CRC document 2023/1.

Financial support. The Geological Survey of South Australia and the MinEx CRC funded this research. This research was supported by an Australian Government Research Training Program (RTP) Scholarship awarded to JCL.

Code availability. R code used to generate the zircon geochemistry plots is available on GitHub at <https://github.com/jarredclloyd/zircon-trace-element-plots>. PowerShell module used to adjust headers for rho calculation is available on GitHub at https://github.com/jarredclloyd/PowerShell_LADR_errorcorrelation_workaround

CRedit author statement. **Jarred C. Lloyd:** Conceptualization, investigation, writing – original draft, writing – review and editing, methodology, formal analysis, data curation and visualization. **Wolfgang V. Preiss:** Investigation and writing – review and editing. **Alan S. Collins:** Conceptualization, funding acquisition, supervision, investigation, and writing – review and editing. **Georgina M. Virgo:** Investigation and writing – review and editing. **Morgan L. Blades:** Investigation and writing – review and editing. **Sarah E. Gilbert:** Formal analysis, methodology, investigation and writing – review and editing. **Darwinaji Subarkah:** Investigation and writing – review and editing. **Carmen B. E. Krapf:** Investigation, writing – review and editing and funding acquisition. **Kathryn J. Amos:** Conceptualization, supervision and writing – review and editing.

References

- Abd El-Rahman Y, Gutzmer J, Li X-H, Seifert T, Li C-F, Ling X-X and Li J (2020) Not all Neoproterozoic iron formations are glaciogenic: Sturtian-aged non-Rapitan exhalative iron formations from the Arabian–Nubian Shield. *Mineralium Deposita* 55, 577–96. doi: [10.1007/s00126-019-00898-0](https://doi.org/10.1007/s00126-019-00898-0).
- Aleinikoff JN, Zartman RE, Walter M, Rankin DW, Lyttle PT and Burton WC (1995) U–Pb ages of metarhyolites of the Catocin and Mount Rogers formations, Central and Southern Appalachians; evidence for two pulses of Iapetan rifting. *American Journal of Science* 295, 428. doi: [10.2475/ajs.295.4.428](https://doi.org/10.2475/ajs.295.4.428).
- Allen PA and Etienne JL (2008) Sedimentary challenge to Snowball Earth. *Nature Geoscience* 1, 817–25. doi: [10.1038/ngeo355](https://doi.org/10.1038/ngeo355).
- Ambrose GJ, Flint RB and Webb AW (1981) *Precambrian and Palaeozoic Geology of the Peake and Denison Ranges*. Bulletin 50. Adelaide, South Australia: Geological Survey of South Australia.
- Anenburg M (2020) Rare earth mineral diversity controlled by REE pattern shapes. *Mineralogical Magazine* 84, 629–39. doi: [10.1180/mgm.2020.70](https://doi.org/10.1180/mgm.2020.70).
- Armistead SE, Collins AS, Buckman S and Atkins R (2020) Age and geochemistry of the Boucaut Volcanics in the Neoproterozoic Adelaide Rift Complex, South Australia. *Australian Journal of Earth Sciences*, 1–10. doi: [10.1080/08120099.2021.1840435](https://doi.org/10.1080/08120099.2021.1840435).
- Arnaud E, Halverson GP and Shields-Zhou GA, eds. (2011) *The Geological Record of Neoproterozoic Glaciations*: Geological Society, Memoirs 36. doi: [10.1144/M36.0](https://doi.org/10.1144/M36.0).
- Baldwin GJ, Turner EC and Kamber BS (2016) Tectonic controls on distribution and stratigraphy of the Cryogenian Rapitan iron formation, northwestern Canada. *Precambrian Research* 278, 303–22. doi: [10.1016/j.precamres.2016.03.014](https://doi.org/10.1016/j.precamres.2016.03.014).
- Barovich KM and Hand M (2008) Tectonic setting and provenance of the Paleoproterozoic Willyama Supergroup, Curnamona Province, Australia: geochemical and Nd isotopic constraints on contrasting source terrain components. *Precambrian Research* 166, 318–37. doi: [10.1016/j.precamres.2007.06.024](https://doi.org/10.1016/j.precamres.2007.06.024).
- Belousova EA, Reid AJ, Griffin WL and O'Reilly SY (2009) Rejuvenation vs. recycling of Archean crust in the Gawler Craton, South Australia: evidence from U–Pb and Hf isotopes in detrital zircon. *Lithos* 113, 570–82. doi: [10.1016/j.lithos.2009.06.028](https://doi.org/10.1016/j.lithos.2009.06.028).
- Belperio AP (1973) *The Stratigraphy and Facies of the Late Precambrian Lower Glacial sequence, Mt Painter, South Australia*. Honours Thesis, Department of Geology, University of Adelaide, Adelaide, South Australia. Published thesis. <https://hdl.handle.net/2440/131123>
- Borg G, Kärner K, Buxton M, Armstrong R and Merwe SWvd (2003) Geology of the Skorpion supergene zinc deposit, Southern Namibia. *Economic Geology* 98, 749–71. doi: [10.2113/gsecongeo.98.4.749](https://doi.org/10.2113/gsecongeo.98.4.749).
- Bowring SA, Grotzinger JP, Condon DJ, Ramezani J, Newall MJ and Allen PA (2007) Geochronologic constraints on the chronostratigraphic framework of the Neoproterozoic Huqf Supergroup, Sultanate of Oman. *American Journal of Science* 307, 1097–145. doi: [10.2475/10.2007.01](https://doi.org/10.2475/10.2007.01).
- Brocks JJ (2018) The transition from a cyanobacterial to algal world and the emergence of animals. *Emerging Topics in Life Sciences* 2, 181–90. doi: [10.1042/etls20180039](https://doi.org/10.1042/etls20180039).
- Callen RA (1990) *Curnamona. 1:250 000 Geological Series—Explanatory Notes*: Department of Mines and Energy. <https://sarigbasis.pir.sa.gov.au/WebtopEw/ws/samref/sarig1/wci/Record?r=0&m=1&w=catno=2021449>
- Calver CR, Crowley JL, Wingate MTD, Evans DAD, Raub TD and Schmitz MD (2013) Globally synchronous Marinoan deglaciation indicated by U–Pb geochronology of the Cottons Breccia, Tasmania, Australia. *Geology* 41, 1127–30. doi: [10.1130/g34568.1](https://doi.org/10.1130/g34568.1).
- Chongyu Y, Feng T, Liu Y, Gao L, Yang Z, Wang Z, Liu 刘鹏举 P, Xing YZ and Song B (2005) New U–Pb zircon ages from the Ediacaran (Sinian) system in the Yangtze Gorges: Constraint on the age of Miaohu biota and Marinoan glaciation. *Geological Bulletin of China* 24, 393–400.
- Coats RP and Forbes BG (1977) Evidence for two Sturtian Glaciations in South Australia. *Quarterly Geological Notes* 64, 19–20. <https://sarigbasis.pir.sa.gov.au/WebtopEw/ws/samref/sarig1/wci/Record?r=0&m=1&w=catno=2041398>
- Coats RP and Preiss WV (1987) Stratigraphy of the Umberatana Group. In *Adelaide Geosyncline—Late Proterozoic Stratigraphy, Sedimentation, Palaeontology and Tectonics* (ed WV Preiss), pp. 125–211. Adelaide, South Australia: Geological Survey of South Australia.
- Collins AS, Reddy SM, Buchan C and Mruma A (2004) Temporal constraints on Palaeoproterozoic eclogite formation and exhumation (Usagaran Orogen, Tanzania). *Earth and Planetary Science Letters* 224, 175–92. doi: [10.1016/j.epsl.2004.04.027](https://doi.org/10.1016/j.epsl.2004.04.027).
- Condon DJ and Bowring SA (2011) A user's guide to Neoproterozoic geochronology. In *The Geological Record of Neoproterozoic Glaciations* (eds E Arnaud, GP Halverson and GA Shields-Zhou), 36, pp. 135–49: Geological Society, Memoirs. doi: [10.1144/m36.9](https://doi.org/10.1144/m36.9).
- Conor CHH and Preiss WV (2008) Understanding the 1720–1640Ma Palaeoproterozoic Willyama Supergroup, Curnamona Province, Southeastern Australia: implications for tectonics, basin evolution and ore genesis. *Precambrian Research* 166, 297–317. doi: [10.1016/j.precamres.2007.08.020](https://doi.org/10.1016/j.precamres.2007.08.020).
- Conor CHH and Preiss WV (2019) Cryogenian glaciomarine megaclasts of the MacDonald Corridor, Bimbowrie Conservation Park, Olary Region, South Australia. *Australian Journal of Earth Sciences* 67, 857–72. doi: [10.1080/08120099.2018.1553206](https://doi.org/10.1080/08120099.2018.1553206).
- Cooper BJ (2010) 'Snowball Earth': the early contribution from South Australia. *Earth Sciences History* 29, 121–45. doi: [10.17704/eshi.29.1.j8874825610u68w5](https://doi.org/10.17704/eshi.29.1.j8874825610u68w5).
- Cooper PF (1973) Striated pebbles from the late Precambrian Adelaidean. *Quarterly Notes – Geological Survey of New South Wales* 11, 13–5.
- Cooper PF and Tuckwell KD (1971) The upper Precambrian Adelaidean of the Broken Hill area—a new subdivision. *Quarterly Notes – Geological Survey of New South Wales* 3, 8–16.
- Cooper PF, Tuckwell KD, Gilligan LB and Meares RMD (1974) *Geology of the Torrowangee and Fowlers Gap 1:100,000 Sheets*. Sydney, New South Wales: Geological Survey of New South Wales, Department of Mines.
- Counts JW (2017) *The Adelaide Rift Complex in the Flinders Ranges: Geologic History, Past Investigations and Relevant Analogues*. Report Book 2017/00016. Adelaide, South Australia: Geological Survey of South Australia, Department of Premier and Cabinet. <https://sarigbasis.pir.sa.gov.au/WebtopEw/ws/samref/sarig1/wcir/Record?r=0&m=1&w=catno=2039731>
- Cowley WM (2020) Geological setting of exceptional geological features of the Flinders Ranges. *Australian Journal of Earth Sciences* 67, 763–85. doi: [10.1080/08120099.2020.1748109](https://doi.org/10.1080/08120099.2020.1748109).
- Cox GM, Halverson GP, Denyszyn S, Foden J and Macdonald FA (2018a) Cryogenian magmatism along the north-western margin of Laurentia: Plume or rift? *Precambrian Research* 319, 144–57. doi: [10.1016/j.precamres.2017.09.025](https://doi.org/10.1016/j.precamres.2017.09.025).
- Cox GM, Halverson GP, Minarik WG, Le Heron DP, Macdonald FA, Bellefroid EJ and Strauss JV (2013) Neoproterozoic iron formation: an

- evaluation of its temporal, environmental and tectonic significance. *Chemical Geology* **362**, 232–49. doi: [10.1016/j.chemgeo.2013.08.002](https://doi.org/10.1016/j.chemgeo.2013.08.002).
- Cox GM, Isakson V, Hoffman PF, Gernon TM, Schmitz MD, Shahin S, Collins AS, Preiss WV, Blades ML, Mitchell RN and Nordsvan A** (2018b) South Australian U–Pb zircon (CA-ID-TIMS) age supports globally synchronous Sturtian deglaciation. *Precambrian Research* **315**, 257–63. doi: [10.1016/j.precamres.2018.07.007](https://doi.org/10.1016/j.precamres.2018.07.007).
- Cox GM, Strauss JV, Halverson GP, Schmitz MD, McClelland WC, Stevenson RS and Macdonald FA** (2015) Kikiktat volcanics of Arctic Alaska—melting of harzburgitic mantle associated with the Franklin large igneous province. *Lithosphere* **7**, 275–95. doi: [10.1130/1435.1](https://doi.org/10.1130/1435.1).
- Cramer F, Shephard GE and Heron PJ** (2020) The misuse of colour in science communication. *Nature Communications* **11**, 5444. doi: [10.1038/s41467-020-19160-7](https://doi.org/10.1038/s41467-020-19160-7).
- Dalgarno CR and Johnson JE** (1966) *Parachilna map sheet SH54-13*, 1st ed. *Geological Atlas of South Australia, 1:250 000 series*. Adelaide, South Australia: Geological Survey of South Australia.
- David TWE** (1906) Australis: les conditions du climat aux époques géologiques. In *10th International Geological Congress*, pp. 275–298. Mexico.
- Deepak A, Löhr S, Abbot AN, Han S, Wheeler C and Sharma M** (2022) *Testing the Precambrian Reverse Weathering Hypothesis Using a 1-Billion-Year Record of Marine Shales*. Honolulu, Hawaii, USA: Goldschmidt. <https://doi.org/10.46427/gold2022.10825>
- Dempster TJ, Rogers G, Tanner PWG, Bluck BJ, Muir RJ, Redwood SD, Ireland TR and Paterson BA** (2002) Timing of deposition, orogenesis and glaciation within the Dalradian rocks of Scotland: constraints from U–Pb zircon ages. *Journal of the Geological Society* **159**, 83–94. doi: [10.1144/0016-764901061](https://doi.org/10.1144/0016-764901061).
- Denyszyn SW, Davis DW and Halls HC** (2009) Paleomagnetism and U–Pb geochronology of the Clarence Head dykes, Arctic Canada: orthogonal emplacement of mafic dykes in a large igneous province. *Canadian Journal of Earth Sciences* **46**, 155–67. doi: [10.1139/E09-011](https://doi.org/10.1139/E09-011).
- Denyszyn SW, Halls HC, Davis DW and Evans DAD** (2009) Paleomagnetism and U–Pb geochronology of Franklin dykes in High Arctic Canada and Greenland: a revised age and paleomagnetic pole constraining block rotations in the Nares Strait region. *Canadian Journal of Earth Sciences* **46**, 689–705. doi: [10.1139/E09-042](https://doi.org/10.1139/E09-042).
- Drexel JF and Preiss WV**, eds. (1995) *The Geology of South Australia*, Bulletin 54. Adelaide, South Australia: Geological Survey of South Australia.
- Dunn PR, Thomson BP and Rankama K** (1971) Late pre-Cambrian glaciation in Australia as a stratigraphic boundary. *Nature* **231**, 498–502. doi: [10.1038/231498a0](https://doi.org/10.1038/231498a0).
- Dyson IA** (1996) Stratigraphy of the Burra and Umberatana Groups in the Willippa Anticline, central Flinders Ranges. *Quarterly Geological Notes* **129**, 10–26.
- Dyson IA** (2004) Geology of the eastern Willouran Ranges – evidence for earliest onset of salt tectonics in the Adelaide Geosyncline. *MESA Journal* **35**, 46–56. <https://sarigbasis.pir.sa.gov.au/WebtopEw/ws/samref/sarig1/wci/Record?r=0&m=1&w=catno=2023965>
- Edgoose CJ** (2013) Chapter 23: Amadeus Basin. In *Geology and Mineral Resources of the Northern Territory* (eds M Ahmad and TJ Munson): Northern Territory Geological Survey, Special Publication 5.
- Eyles N and Januszczak N** (2004) ‘Zipper-rift’: a tectonic model for Neoproterozoic glaciations during the breakup of Rodinia after 750 Ma. *Earth-Science Reviews* **65**, 1–73. doi: [10.1016/s0012-8252\(03\)00080-1](https://doi.org/10.1016/s0012-8252(03)00080-1).
- Eyster A, Ferri F, Schmitz MD and Macdonald FA** (2018) One diamictite and two rifts: Stratigraphy and geochronology of the Gataga Mountain of northern British Columbia. *American Journal of Science* **318**, 167–207. doi: [10.2475/02.2018.1](https://doi.org/10.2475/02.2018.1).
- Fabris AJ, Constable SA, Conor CHH, Woodhouse A, Hore SB and Fanning M** (2005) Age, origin, emplacement and mineral potential of the Oodla Wirra Volcanics, Nackara Arc, central Flinders Ranges. *MESA Journal* **37**, 44–52. <https://sarigbasis.pir.sa.gov.au/WebtopEw/ws/samref/sarig1/wci/Record?r=0&m=1&w=catno=2025119>
- Fairchild IJ and Kennedy MJ** (2007) Neoproterozoic glaciation in the earth system. *Journal of the Geological Society* **164**, 895–921. doi: [10.1144/0016-76492006-191](https://doi.org/10.1144/0016-76492006-191).
- Fanning CM and Link PK** (2004) U–Pb SHRIMP ages of Neoproterozoic (Sturtian) glaciogenic Pocatello Formation, southeastern Idaho. *Geology* **32**, 881–4. doi: [10.1130/G20609.1](https://doi.org/10.1130/G20609.1).
- Fanning CM and Link PK** (2006) Constraints on the timing of the Sturtian Glaciation from Southern Australia; IE for the true Sturtian. In *2006 Philadelphia Annual Meeting*, vol. 7, p. 115: Geological Society of America, Abstracts with Programs 38. https://gsa.confex.com/gsa/2006AM/finalprogram/abstract_116074.htm
- Fanning CM and Link PK** (2008) Age constraints for the Sturtian Glaciation; data from the Adelaide Geosyncline, South Australia and Pocatello Formation, Idaho, USA. In *Neoproterozoic extreme climates and the origin of early metazoan life, Selwyn Symposium of the GSA Victoria Division*, The University of Melbourne, pp. 57–62. Melbourne, Victoria: Geological Society of Australia.
- Fanning CM, Reid AJ and Teale GS** (2007) *A Geochronological Framework for the Gawler Craton, South Australia*. Bulletin 55, p. 258. Adelaide, South Australia: Geological Survey of South Australia.
- Fergusson CL, Henderson RA, Fanning CM and Withnall IW** (2007) Detrital zircon ages in Neoproterozoic to Ordovician siliciclastic rocks, northeastern Australia: implications for the tectonic history of the East Gondwana continental margin. *Journal of the Geological Society* **164**, 215–25. doi: [10.1144/0016-76492005-136](https://doi.org/10.1144/0016-76492005-136).
- Fetter AH and Goldberg SA** (1995) Age and geochemical characteristics of bimodal magmatism in the Neoproterozoic Grandfather Mountain Rift Basin. *The Journal of Geology* **103**, 313–26. doi: [10.1086/629749](https://doi.org/10.1086/629749).
- Fioretti AM, Black LP, Foden J and Visonà D** (2005) Grenville-age magmatism at the South Tasman Rise (Australia): a new piercing point for the reconstruction of Rodinia. *Geology* **33**, 769–72. doi: [10.1130/G21671.1](https://doi.org/10.1130/G21671.1).
- Fitzherbert JA and Downes PM** (2015) A concise geological history of the Broken Hill region. *Quarterly Notes – Geological Survey of New South Wales* **143**, 29–43.
- Foden JD, Elburg MA, Dougherty-Page J and Burtt A** (2006) The timing and duration of the Delamerian orogeny: correlation with the Ross Orogen and implications for Gondwana assembly. *Journal of Geology* **114**, 189–210. doi: [10.1086/499570](https://doi.org/10.1086/499570).
- Foden JD, Elburg MA, Turner S, Clark C, Blades ML, Cox G, Collins AS, Wolff K and George C** (2020) Cambro-Ordovician magmatism in the Delamerian orogeny: implications for tectonic development of the southern Gondwanan margin. *Gondwana Research* **81**, 490–521. doi: [10.1016/j.gr.2019.12.006](https://doi.org/10.1016/j.gr.2019.12.006).
- Forbes BG** (1971) *Parachilna. 1:250 000 Geological Series—Explanatory Notes*. Adelaide, South Australia: Department of Mines South Australia.
- Forbes BG and Cooper RS** (1976) The Pualco Tillite of the Olary Region, South Australia. *Quarterly Geological Notes* **60**, 2–5.
- Fraser GL, McAvaney S, Neumann NL, Szpunar M and Reid A** (2010) Discovery of early Mesoproterozoic crust in the eastern Gawler Craton, South Australia. *Precambrian Research* **179**, 1–21. doi: [10.1016/j.precamres.2010.02.008](https://doi.org/10.1016/j.precamres.2010.02.008).
- Fraser GL and Neumann NL** (2010) *New SHRIMP U–Pb zircon Ages from the Gawler Craton and Curnamona Province, South Australia, 2008–2010*. Record 2010/16. Canberra: Geoscience Australia, G Australia. <http://pid.geoscience.gov.au/dataset/ga/70348>
- Frimmel HE, Klötzli US and Siegfried PR** (1996) New Pb–Pb single zircon age constraints on the timing of Neoproterozoic glaciation and continental Break-up in Namibia. *The Journal of Geology* **104**, 459–69. doi: [10.1086/629839](https://doi.org/10.1086/629839).
- Frimmel HE, Zartman RE and Späth A** (2001) The Richtersveld Igneous complex, South Africa: U–Pb zircon and geochemical evidence for the beginning of Neoproterozoic continental breakup. *The Journal of Geology* **109**, 493–508. doi: [10.1086/320795](https://doi.org/10.1086/320795).
- Gehrels GE, Valencia VA and Ruiz J** (2008) Enhanced precision, accuracy, efficiency, and spatial resolution of U–Pb ages by laser ablation-multi-collector-inductively coupled plasma-mass spectrometry. *Geochemistry, Geophysics, Geosystems* **9**. doi: [10.1029/2007gc001805](https://doi.org/10.1029/2007gc001805).
- Govindaraju K** (1995) 1995 working values with confidence limits for twenty-six CRPG, ANRT and IWG-GIT geostandards. *Geostandards Newsletter* **19** (s1), 1–32. doi: [10.1111/j.1751-908X.1995.tb00164.x](https://doi.org/10.1111/j.1751-908X.1995.tb00164.x).

- Gradstein FM, Ogg JG and Smith AG, eds. (2005) *A Geologic Time Scale 2004*. Cambridge University Press. doi: [10.1017/CBO9780511536045](https://doi.org/10.1017/CBO9780511536045).
- Grimes CB, John BE, Kelemen PB, Mazdab FK, Wooden JL, Cheadle MJ, Hanghøj K and Schwartz JJ (2007) Trace element chemistry of zircons from oceanic crust: A method for distinguishing detrital zircon provenance. *Geology* **35**, 643–46. doi: [10.1130/G23603A.1](https://doi.org/10.1130/G23603A.1).
- Grimes CB, Wooden JL, Cheadle MJ and John BE (2015) “Fingerprinting” tectono-magmatic provenance using trace elements in igneous zircon. *Contributions to Mineralogy and Petrology* **170**, 46. doi: [10.1007/s00410-015-1199-3](https://doi.org/10.1007/s00410-015-1199-3).
- Halverson GP, Hurtgen MT, Porter SM and Collins AS (2009) Neoproterozoic-Cambrian biogeochemical evolution. In *Developments in Precambrian Geology* (eds C Gaucher, AN Sial, HE Frimmel and GP Halverson), vol. **16**, pp. 351–65: Elsevier. doi: [10.1016/S0166-2635\(09\)01625-9](https://doi.org/10.1016/S0166-2635(09)01625-9).
- Halverson GP, Porter SM and Gibson TM (2018) Dating the late Proterozoic stratigraphic record. *Emerging Topics in Life Sciences* **2**, 137–47. doi: [10.1042/etls20170167](https://doi.org/10.1042/etls20170167).
- Harland WB (1964) Critical evidence for a great infra-Cambrian glaciation. *Geologische Rundschau* **54**, 45–61. doi: [10.1007/BF01821169](https://doi.org/10.1007/BF01821169).
- He J, Zhu W and Ge R (2014) New age constraints on Neoproterozoic diamictites in Kuruktag, NW China and Precambrian crustal evolution of the Tarim Craton. *Precambrian Research* **241**, 44–60. doi: [10.1016/j.precamres.2013.11.005](https://doi.org/10.1016/j.precamres.2013.11.005).
- Hoffman PF (2011) A history of Neoproterozoic glacial geology, 1871–1997. In *The Geological Record of Neoproterozoic Glaciations* (eds E Arnaud, GP Halverson and GA Shields-Zhou), pp. 17–37: Geological Society, Memoirs **36**. doi: [10.1144/m36.2](https://doi.org/10.1144/m36.2).
- Hoffman PF, Abbot DS, Ashkenazy Y, Benn DI, Brocks JJ, Cohen PA, Cox GM, Creveling JR, Donnadieu Y, Erwin DH, Fairchild IJ, Ferreira D, Goodman JC, Halverson GP, Jansen MF, Le Hir G, Love GD, Macdonald FA, Maloof AC, Partin CA, Ramstein G, Rose BEJ, Rose CV, Sadler PM, Tziperman E, Voigt A and Warren SG (2017) Snowball Earth climate dynamics and Cryogenian geology-geobiology. *Science Advances* **3**, e1600983. doi: [10.1126/sciadv.1600983](https://doi.org/10.1126/sciadv.1600983).
- Hoffman PF, Hawkins D, Isachsen C and Bowring SA (1996) Precise U–Pb zircon ages for early Damaran magmatism in the Summas Mountains and Welwitschia Inlier, northern Damara belt, Namibia. *Communications of the Geological Survey of Namibia* **11**, 47–52.
- Hoffman PF, Kaufman AJ, Halverson GP and Schrag DP (1998) A Neoproterozoic Snowball earth. *Science* **281**, 1342. doi: [10.1126/science.281.5381.1342](https://doi.org/10.1126/science.281.5381.1342).
- Hoffman PF and Schrag DP (2002) The snowball earth hypothesis: testing the limits of global change. *Terra Nova* **14**, 129–55. doi: [10.1046/j.1365-3121.2002.00408.x](https://doi.org/10.1046/j.1365-3121.2002.00408.x).
- Hogmalm KJ, Zack T, Karlsson AKO, Sjöqvist ASL and Garbe-Schönberg D (2017) In situ Rb–Sr and K–Ca dating by LA-ICP-MS/MS: an evaluation of N₂O and SF₆ as reaction gases. *Journal of Analytical Atomic Spectrometry* **32**, 305–13. doi: [10.1039/c6ja00362a](https://doi.org/10.1039/c6ja00362a).
- Hood AvS, Penman DE, Lechte MA, Wallace MW, Giddings JA and Planavsky NJ (2021) Neoproterozoic syn-glacial carbonate precipitation and implications for a snowball Earth. *Geobiology*. doi: [10.1111/gbi.12470](https://doi.org/10.1111/gbi.12470).
- Hopton DL (1983) *Environmental analysis of the Late Precambrian Appila Tillite equivalent at Depot Flat, southern Flinders Ranges, South Australia*. Honours Thesis, Department of Geology and Mineralogy, University of Adelaide, Adelaide, South Australia. Published thesis. <https://hdl.handle.net/2440/131612>
- Horstwood MSA, Kosler J, Gehrels GE, Jackson SE, McLean NM, Paton C, Pearson NJ, Sircombe KN, Sylvester P, Vermeesch P, Bowring JF, Condon DJ and Schoene B (2016) Community-derived standards for LA-ICP-MS U-(Th)-Pb geochronology – uncertainty propagation, age interpretation and data reporting. *Geostandards and Geoanalytical Research* **40**, 311–32. doi: [10.1111/j.1751-908X.2016.00379.x](https://doi.org/10.1111/j.1751-908X.2016.00379.x).
- Hoskin PWO and Ireland TR (2000) Rare earth element chemistry of zircon and its use as a provenance indicator. *Geology* **28**, 627–30. doi: [10.1130/0091-7613\(2000\)28<627:REECOZ>2.0.CO;2](https://doi.org/10.1130/0091-7613(2000)28<627:REECOZ>2.0.CO;2).
- Hoskin PWO and Schaltegger U (2003) The composition of zircon and igneous and metamorphic petrogenesis. *Reviews in Mineralogy and Geochemistry* **53**, 27–62. doi: [10.2113/0530027](https://doi.org/10.2113/0530027).
- Howchin W (1901) Preliminary note on the existence of Glacial Beds of Cambrian Age in South Australia. *Transactions of the Royal Society of South Australia* **25**, 10–3.
- Howchin W (1904) The geology of the Mount Lofty Ranges: part I. *Transactions of the Royal Society of South Australia* **28**, 253–80.
- Howchin W (1906) The geology of the Mount Lofty Ranges: part II. *Transactions of the Royal Society of South Australia* **30**, 227–62.
- Howchin W (1908) Glacial beds of Cambrian age in South Australia. *Quarterly Journal of the Geological Society* **64**, 234. doi: [10.1144/GSL.JGS.1908.064.01-04.13](https://doi.org/10.1144/GSL.JGS.1908.064.01-04.13).
- Howchin W (1920) Past glacial action in Australia. In *Year Book* (ed Australian Bureau of Statistics), vol. **13**, pp. 1133–46. Melbourne, Victoria: Australian Bureau of Statistics.
- Ireland TR, Flöttmann T, Fanning CM, Gibson GM and Preiss WV (1998) Development of the early Paleozoic Pacific margin of Gondwana from detrital-zircon ages across the Delamerian orogen. *Geology* **26**, 243–46. doi: [10.1130/0091-7613\(1998\)026<0243:Dotepp>2.3.Co;2](https://doi.org/10.1130/0091-7613(1998)026<0243:Dotepp>2.3.Co;2).
- Isakson VH (2017) *Geochronology of the Tectonic, Stratigraphic, and Magmatic Evolution of Neoproterozoic to Early Paleozoic, North American Cordillera and Cryogenian Glaciation*. Dissertation, Department of Geoscience, Boise State University, Boise, Idaho, USA. Published thesis. doi: [10.18122/B2P42Z](https://doi.org/10.18122/B2P42Z).
- Jackson SE, Pearson NJ, Griffin WL and Belousova EA (2004) The application of laser ablation-inductively coupled plasma-mass spectrometry to in situ U–Pb zircon geochronology. *Chemical Geology* **211**, 47–69. doi: [10.1016/j.chemgeo.2004.06.017](https://doi.org/10.1016/j.chemgeo.2004.06.017).
- Jacobs J, Elburg MA, Läufer A, Kleinhanns IC, Henjes-Kunst F, Estrada S, Ruppel AS, Damaske D, Montero P and Bea F (2015) Two distinct Late Mesoproterozoic/Early Neoproterozoic basement provinces in central/eastern Dronning Maud Land, East Antarctica: the missing link, 15–21°E. *Precambrian Research* **265**, 249–72. doi: [10.1016/j.precamres.2015.05.003](https://doi.org/10.1016/j.precamres.2015.05.003).
- Jagodzinski EA and Fricke CE (2010) *Compilation of New SHRIMP U-Pb geochronological data for the Southern Curnamona Province, South Australia, 2010*. Report Book 2010/00014. Adelaide, South Australia: Geological Survey of South Australia, Department of Primary Industries and Resources.
- Jagodzinski EA and McAvaney SO (2017) *SHRIMP U-Pb Geochronology Data for Northern Eyre Peninsula, 2014–2016*. Report Book 2016/00001. Adelaide, South Australia: Geological Survey of South Australia, Department of Premier and Cabinet. <https://sarigbasis.pir.sa.gov.au/WebtopEw/ws/samref/sarig1/wci/Record?r=0&m=1&w=catno=2039475>
- Jagodzinski EA, Werner M, Curtis S, Fabris A, Pawley M and Krapf C (2020) *SHRIMP Geochronology of the Mt Double Area, Southern Gawler Ranges Margin*. Report Book 2020/00006. South Australia: Geological Survey of South Australia, Department for Energy and Mining. doi: [10.13140/RG.2.17511.47523](https://doi.org/10.13140/RG.2.17511.47523).
- Jefferson CW and Parrish RR (1989) Late Proterozoic stratigraphy, U–Pb zircon ages, and rift tectonics, Mackenzie Mountains, northwestern Canada. *Canadian Journal of Earth Sciences* **26**, 1784–801. doi: [10.1139/e89-151](https://doi.org/10.1139/e89-151).
- Jochum KP, Weis U, Stoll B, Kuzmin D, Yang Q, Raczek I, Jacob DE, Stracke A, Birbaum K, Frick DA, Günther D and Enzweiler J (2011) Determination of reference values for NIST SRM 610–617 glasses following ISO guidelines. *Geostandards and Geoanalytical Research* **35**, 397–429. doi: [10.1111/j.1751-908X.2011.00120.x](https://doi.org/10.1111/j.1751-908X.2011.00120.x).
- Karlstrom KE, Bowring SA, Dehler CM, Knoll AH, Porter SM, Marais DJD, Weil AB, Sharp ZD, Geissman JW, Elrick MB, Timmons JM, Crossey LJ and Davidek KL (2000) Chuar Group of the Grand Canyon: record of breakup of Rodinia, associated change in the global carbon cycle, and ecosystem expansion by 740 Ma. *Geology* **28**, 619–22. doi: [10.1130/0091-7613\(2000\)28<619:CGOTGC>2.0.CO;2](https://doi.org/10.1130/0091-7613(2000)28<619:CGOTGC>2.0.CO;2).
- Keeley JA, Link PK, Fanning CM and Schmitz MD (2013) Pre- to synglacial rift-related volcanism in the Neoproterozoic (Cryogenian) Pocatello Formation, SE Idaho: new SHRIMP and CA-ID-TIMS constraints. *Lithosphere* **5**, 128–50. doi: [10.1130/L226.1](https://doi.org/10.1130/L226.1).

- Keeman J, Turner S, Haines PW, Belousova E, Ireland T, Brouwer P, Foden J and Wörner G (2020) New UPb, Hf and O isotope constraints on the provenance of sediments from the Adelaide Rift Complex – documenting the key Neoproterozoic to early Cambrian succession. *Gondwana Research* **83**, 248–78. doi: [10.1016/j.gr.2020.02.005](https://doi.org/10.1016/j.gr.2020.02.005).
- Kendall BS, Creaser RA, Calver CR, Raub TD and Evans DAD (2009) Correlation of Sturtian diamictite successions in southern Australia and northwestern Tasmania by Re–Os black shale geochronology and the ambiguity of “Sturtian”-type diamictite–cap carbonate pairs as chronostratigraphic marker horizons. *Precambrian Research* **172**, 301–10. doi: [10.1016/j.precamres.2009.05.001](https://doi.org/10.1016/j.precamres.2009.05.001).
- Kendall BS, Creaser RA, Ross GM and Selby D (2004) Constraints on the timing of Marinoan “Snowball Earth” glaciation by 187Re–187Os dating of a Neoproterozoic, post-glacial black shale in Western Canada. *Earth and Planetary Science Letters* **222**, 729–40. doi: [10.1016/j.epsl.2004.04.004](https://doi.org/10.1016/j.epsl.2004.04.004).
- Kendall BS, Creaser RA and Selby D (2006) Re–Os geochronology of postglacial black shales in Australia: constraints on the timing of “Sturtian” glaciation. *Geology* **34**, 729–32. doi: [10.1130/g22775.1](https://doi.org/10.1130/g22775.1).
- Kennedy K, Eyles N and McArthur A (2020) Syn-rift mass flow generated ‘tectonofacies’ and ‘tectonosequences’ of the Kingston Peak Formation, Death Valley, California, and their bearing on supposed Neoproterozoic panglacial climates. *Sedimentology* **68**, 352–81. doi: [10.1111/sed.12781](https://doi.org/10.1111/sed.12781).
- Key RM, Liyungu AK, Njamu FM, Somwe V, Banda J, Mosley PN and Armstrong RA (2001) The western arm of the Lufilian Arc in NW Zambia and its potential for copper mineralization. *Journal of African Earth Sciences* **33**, 503–28. doi: [10.1016/S0899-5362\(01\)00098-7](https://doi.org/10.1016/S0899-5362(01)00098-7).
- Kirschvink JL (1992) Late Proterozoic Low-Latitude Global Glaciation: the Snowball earth (eds JW Schopf and C Klein), pp. 51–2. Cambridge University Press. <https://resolver.caltech.edu/CaltechAUTHORS:20130117-100718783>
- Knoll AH, Walter MR, Narbonne GM and Christie-Blick N (2006) The Ediacaran Period: a new addition to the geologic time scale. *Lethaia* **39**, 13–30. doi: [10.1080/00241160500409223](https://doi.org/10.1080/00241160500409223).
- Kochnev BB, Pokrovskii BG and Proshenkin AI (2015) The upper Neoproterozoic glacial complex in central areas of the Siberian platform. *Doklady Earth Sciences* **464**, 1001–4. doi: [10.1134/s1028334x15100049](https://doi.org/10.1134/s1028334x15100049).
- Korsch RJ, Huston DL, Henderson RA, Blewett RS, Withnall IW, Fergusson CL, Collins WJ, Saygin E, Kositcin N, Meixner AJ, Chopping R, Henson PA, Champion DC, Hutton LJ, Wormald R, Holzschuh J and Costelloe RD (2012) Crustal architecture and geodynamics of North Queensland, Australia: insights from deep seismic reflection profiling. *Tectonophysics* **572–573**, 76–99. doi: [10.1016/j.tecto.2012.02.022](https://doi.org/10.1016/j.tecto.2012.02.022).
- Krasnobaev AA, Puchkov VN, Sergeeva ND and Busharina SV (2019) Nature of zircon clastics in the Riphean and Vendian sandstones of the Southern Urals. *Georesursy* **21**, 15–25. doi: [10.18599/grs.2019.1.15-25](https://doi.org/10.18599/grs.2019.1.15-25).
- Kromkhun K, Foden JD, Hore SB and Baines G (2013) Geochronology and Hf isotopes of the bimodal mafic–felsic high heat producing igneous suite from Mt Painter Province, South Australia. *Gondwana Research* **24**, 1067–79. doi: [10.1016/j.gr.2013.01.011](https://doi.org/10.1016/j.gr.2013.01.011).
- Kruse PD, Dunster JN and Munson TJ (2013) Chapter 28: Georgina Basin. In *Geology and Mineral Resources of the Northern Territory* (eds M Ahmad and TJ Munson), pp. 28:1–28:56. Northern Territory: Northern Territory Geological Survey, Special Publication 5.
- Lamothe KG, Hoffman PF, Greenman JW and Halverson GP (2019) Stratigraphy and isotope geochemistry of the pre-Sturtian Ugab Subgroup, Otavi/Swakop Group, northwestern Namibia. *Precambrian Research* **332**, 105387. doi: [10.1016/j.precamres.2019.105387](https://doi.org/10.1016/j.precamres.2019.105387).
- Lan Z, Huyskens MH, Lu K, Li X-H, Zhang G, Lu D and Yin Q-Z (2020) Toward refining the onset age of Sturtian glaciation in South China. *Precambrian Research* **338**. doi: [10.1016/j.precamres.2019.105555](https://doi.org/10.1016/j.precamres.2019.105555).
- Lan Z, Li X, Zhu M, Chen Z-Q, Zhang Q, Li Q, Lu D, Liu Y and Tang G (2014) A rapid and synchronous initiation of the wide spread Cryogenian glaciations. *Precambrian Research* **255**, 401–11. doi: [10.1016/j.precamres.2014.10.015](https://doi.org/10.1016/j.precamres.2014.10.015).
- Lan Z, Li X-H, Zhu M, Zhang Q and Li Q-L (2015) Revisiting the Liantuo Formation in Yangtze Block, South China: SIMS U–Pb zircon age constraints and regional and global significance. *Precambrian Research* **263**, 123–41. doi: [10.1016/j.precamres.2015.03.012](https://doi.org/10.1016/j.precamres.2015.03.012).
- Le Heron DP (2012) The Cryogenian record of glaciation and deglaciation in South Australia. *Sedimentary Geology* **243–244**, 57–69. doi: [10.1016/j.sedgeo.2011.09.013](https://doi.org/10.1016/j.sedgeo.2011.09.013).
- Le Heron DP, Busfield ME and Collins AS (2014) Bolla Bollana boulder beds: a Neoproterozoic trough mouth fan in South Australia? *Sedimentology* **61**, 978–95. doi: [10.1111/sed.12082](https://doi.org/10.1111/sed.12082).
- Le Heron DP, Cox GM, Trundle A and Collins AS (2011) Two Cryogenian glacial successions compared: aspects of the Sturt and Elatina sediment records of South Australia. *Precambrian Research* **186**, 147–68. doi: [10.1016/j.precamres.2011.01.014](https://doi.org/10.1016/j.precamres.2011.01.014).
- Le Heron DP, Eyles N and Busfield ME (2020) The Laurentian Neoproterozoic Glacial Interval: reappraising the extent and timing of glaciation. *Austrian Journal of Earth Sciences* **113**, 59–70. doi: [10.17738/ajes.2020.0004](https://doi.org/10.17738/ajes.2020.0004).
- Lechte MA and Wallace MW (2015) Sedimentary and tectonic history of the Holowilena Ironstone, a Neoproterozoic iron formation in South Australia. *Sedimentary Geology* **329**, 211–24. doi: [10.1016/j.sedgeo.2015.09.014](https://doi.org/10.1016/j.sedgeo.2015.09.014).
- Lechte MA, Wallace MW, Hood AvS, Li W, Jiang G, Halverson GP, Asael D, McColl SL and Planavsky NJ (2019) Subglacial meltwater supported aerobic marine habitats during Snowball Earth. *Proc Natl Acad Sci USA* **116**, 25478–83. doi: [10.1073/pnas.1909165116](https://doi.org/10.1073/pnas.1909165116).
- Lechte MA, Wallace MW, Hood AvS and Planavsky N (2018) Cryogenian iron formations in the glaciogenic Kingston Peak Formation, California. *Precambrian Research* **310**, 443–62. doi: [10.1016/j.precamres.2018.04.003](https://doi.org/10.1016/j.precamres.2018.04.003).
- Li XH, Abd El-Rahman Y, Abu Anbar M, Li J, Ling XX, Wu LG and Masoud AE (2018) Old continental crust underlying juvenile oceanic arc: evidence from Northern Arabian–Nubian Shield, Egypt. *Geophysical Research Letters* **45**, 3001–8. doi: [10.1002/2018gl077121](https://doi.org/10.1002/2018gl077121).
- Li Z-X and Evans DAD (2010) Late Neoproterozoic 40 intraplate rotation within Australia allows for a tighter-fitting and longer-lasting Rodinia. *Geology* **39**, 39–42. doi: [10.1130/g31461.1](https://doi.org/10.1130/g31461.1).
- Link PK (1977) *Facies and Palaeogeography of Late Precambrian Sturtian Glacial Sediments, Copley Area, Northern Flinders Ranges and in the Sturt Gorge near Adelaide, South Australia*. Honours Thesis, Department of Geology and Mineralogy, University of Adelaide, Adelaide. Published thesis. <https://hdl.handle.net/2440/131122>
- Link PK and Gostin VA (1981) Facies and paleogeography of Sturtian glacial strata (late Precambrian), South Australia. *American Journal of Science* **281**, 353. doi: [10.2475/ajs.281.4.353](https://doi.org/10.2475/ajs.281.4.353).
- Lloyd JC, Blades ML, Counts JW, Collins AS, Amos KJ, Wade BP, Hall JW, Hore S, Ball AL, Shahin S and Drabsch M (2020) Neoproterozoic geochronology and provenance of the Adelaide Superbasin. *Precambrian Research* **350**, 105849. doi: [10.1016/j.precamres.2020.105849](https://doi.org/10.1016/j.precamres.2020.105849).
- Lloyd JC, Collins AS, Blades ML, Gilbert SE and Amos KJ (2022) Early evolution of the Adelaide Superbasin. *Geosciences* **12**, 154. doi: [10.3390/geosciences12040154](https://doi.org/10.3390/geosciences12040154).
- Lund K, Aleinikoff JN, Evans KV, duBray EA, Dewitt EH and Unruh DM (2010) SHRIMP U–Pb dating of recurrent Cryogenian and Late Cambrian–early Ordovician alkalic magmatism in central Idaho: implications for Rodinian rift tectonics. *GSA Bulletin* **122**, 430–53. doi: [10.1130/B26565.1](https://doi.org/10.1130/B26565.1).
- Lund K, Aleinikoff JN, Evans KV and Fanning CM (2003) SHRIMP U–Pb geochronology of Neoproterozoic Windermere Supergroup, central Idaho: implications for rifting of western Laurentia and synchronicity of Sturtian glacial deposits. *GSA Bulletin* **115**, 349–72. doi: [10.1130/0016-7606\(2003\)115<0349:SUPGON>2.0.CO;2](https://doi.org/10.1130/0016-7606(2003)115<0349:SUPGON>2.0.CO;2).
- Macdonald FA, Schmitz MD, Crowley JL, Roots CF, Jones DS, Maloof AC, Strauss JV, Cohen PA, Johnston DT and Schrag DP (2010) Calibrating the Cryogenian. *Science* **327**, 1241–43. doi: [10.1126/science.1183325](https://doi.org/10.1126/science.1183325).
- Macdonald FA, Schmitz MD, Strauss JV, Halverson GP, Gibson TM, Eyster A, Cox G, Mamrol P and Crowley JL (2018) Cryogenian of Yukon. *Precambrian Research* **319**, 114–43. doi: [10.1016/j.precamres.2017.08.015](https://doi.org/10.1016/j.precamres.2017.08.015).
- Mackay WG (2011) *Structure and Sedimentology of the Curdimurka Subgroup, Northern Adelaide Fold Belt, South Australia*. Doctoral Thesis, University of Tasmania, Hobart, Tasmania. Published thesis. <https://eprints.utas.edu.au/12486/>
- MacLennan S, Park Y, Swanson-Hysell N, Maloof A, Schoene B, Gebreslassie M, Antilla E, Tesema T, Alene M and Haileab B (2018) The arc of the Snowball: U–Pb dates constrain the Islay anomaly and the initiation of the Sturtian glaciation. *Geology* **46** 539–42. doi: [10.1130/G40171.1](https://doi.org/10.1130/G40171.1).

- Mattinson JM** (2005) Zircon U–Pb chemical abrasion (“CA-TIMS”) method: combined annealing and multi-step partial dissolution analysis for improved precision and accuracy of zircon ages. *Chemical Geology* **220**, 47–66. doi: [10.1016/j.chemgeo.2005.03.011](https://doi.org/10.1016/j.chemgeo.2005.03.011).
- Mawson D and Sprigg RC** (1950) Subdivision of the Adelaide system. *Australian Journal of Science* **13**, 69–72.
- McAvaney SO** (2012) The Cooyerdoo Granite: Paleo- and Mesoarchean basement of the Gawler Craton. *MESA Journal* **65**, 31–40. <https://sarigbasis.pir.sa.gov.au/WebtopEw/ws/samref/sarig1/wci/Record?r=0&m=1&w=catno=2035289>
- McDonough MR and Parrish RR** (1991) Proterozoic gneisses of the Malton complex, near Valemount, British Columbia: U–Pb ages and Nd isotopic signatures. *Canadian Journal of Earth Sciences* **28**, 1202–16. doi: [10.1139/e91-108](https://doi.org/10.1139/e91-108).
- Meaney KJ** (2012) *The Geochronology and Structural Evolution of the Warren Inlier and Springfield Sequence, Mt. Lofty Ranges: Implications for Proterozoic paleogeographic Reconstructions*. Honours Thesis, School of Earth and Environmental Sciences, University of Adelaide, Adelaide, South Australia. Published thesis. <https://hdl.handle.net/2440/95177>
- Meaney KJ** (2017) *Proterozoic Crustal Growth in the Southeastern Gawler Craton: The Development of the Barossa Complex, and an Assessment of the Detrital Zircon Method*. Doctoral Thesis, Department of Geology and Geophysics, University of Adelaide, Adelaide, South Australia. Published thesis. <https://hdl.handle.net/2440/114255>
- Merdith AS, Williams SE, Müller RD and Collins AS** (2017) Kinematic constraints on the Rodinia to Gondwana transition. *Precambrian Research* **299**, 132–50. doi: [10.1016/j.precamres.2017.07.013](https://doi.org/10.1016/j.precamres.2017.07.013).
- Miller RM** (2013) Comparative stratigraphic and geochronological evolution of the Northern Damara Supergroup in Namibia and the Katanga Supergroup in the Lufilian Arc of central Africa. *Geoscience Canada* **40**, 118–40. doi: [10.12789/geocanj.2013.40.007](https://doi.org/10.12789/geocanj.2013.40.007).
- Morrissey LJ, Barovich KM, Hand M, Howard KE and Payne JL** (2019) Magmatism and metamorphism at ca. 1.45 Ga in the northern Gawler Craton: the Australian record of rifting within Nuna (Columbia). *Geoscience Frontiers* **10**, 175–94. doi: [10.1016/j.gsf.2018.07.006](https://doi.org/10.1016/j.gsf.2018.07.006).
- Morrissey LJ, Barovich KM, Hand M, Howard KE, Payne JL and Reid AJ** (2018) The final event in the long evolution of the Gawler Craton: new constraints on 1450 Ma metamorphism and magmatism. *MESA Journal* **88**, 4–11. <https://sarigbasis.pir.sa.gov.au/WebtopEw/ws/samref/sarig1/image/DDD/MESAJ088004-011.pdf>
- Morrissey LJ, Hand M, Wade BP and Szpunar MA** (2013) Early Mesoproterozoic metamorphism in the Barossa Complex, South Australia: links with the eastern margin of Proterozoic Australia. *Australian Journal of Earth Sciences* **60**, 769–95. doi: [10.1080/08120099.2013.860623](https://doi.org/10.1080/08120099.2013.860623).
- Mundil R, Ludwig KR, Metcalfe I and Renne PR** (2004) Age and timing of the Permian mass extinctions: U/Pb dating of closed-system zircons. *Science* **305**, 1760–3. doi: [10.1126/science.1101012](https://doi.org/10.1126/science.1101012).
- Murrell B, Link PK and Gostin VA** (1977) Evidence for only one Sturtian Glacial period in the Copley map area. *Quarterly Geological Notes* **64**, 16–9. <https://sarigbasis.pir.sa.gov.au/WebtopEw/ws/samref/sarig1/wci/Record?r=0&m=1&w=catno=2041398>
- Nascimento DB, Ribeiro A, Trouw RAJ, Schmitt RS and Passchier CW** (2016) Stratigraphy of the Neoproterozoic Damara sequence in northwest Namibia: slope to basin sub-marine mass-transport deposits and olistolith fields. *Precambrian Research* **278**, 108–25. doi: [10.1016/j.precamres.2016.03.005](https://doi.org/10.1016/j.precamres.2016.03.005).
- Nascimento DB, Schmitt RS, Ribeiro A, Trouw RAJ, Passchier CW and Basei MAS** (2017) Depositional ages and provenance of the Neoproterozoic Damara Supergroup (northwest Namibia): implications for the Angola-Congo and Kalahari cratons connection. *Gondwana Research* **52**, 153–71. doi: [10.1016/j.gr.2017.09.006](https://doi.org/10.1016/j.gr.2017.09.006).
- Normington VJ and Donnellan NC** (2020) *Characterisation of the Neoproterozoic Succession of the Northeastern Amadeus Basin, Northern Territory*. Record 2020-010. Northern Territory Geological Survey. <https://sarigbasis.pir.sa.gov.au/WebtopEw/ws/samref/sarig1/wci/Record?r=0&m=1&w=catno=1211>
- Norris A and Danyushevsky L** (2018) *Towards Estimating the Complete Uncertainty Budget of Quantified Results Measured by LA-ICP-MS*, Boston, MA: Goldschmidt.
- O’Neill HSC** (2016) The smoothness and shapes of chondrite-normalized rare earth element patterns in basalts. *Journal of Petrology* **57**, 1463–508. doi: [10.1093/petrology/egw047](https://doi.org/10.1093/petrology/egw047).
- Och LM and Shields-Zhou GA** (2012) The Neoproterozoic oxygenation event: environmental perturbations and biogeochemical cycling. *Earth-Science Reviews* **110**, 26–57. doi: [10.1016/j.earscirev.2011.09.004](https://doi.org/10.1016/j.earscirev.2011.09.004).
- Park Y, Swanson-Hysell NL, MacLennan SA, Maloof AC, Gebreslassie M, Tremblay MM, Schoene B, Alene M, Anttila ESC, Tesema T and Haileab B** (2019) The lead-up to the Sturtian Snowball Earth: neoproterozoic chemostratigraphy time-calibrated by the Tambien Group of Ethiopia. *GSA Bulletin* **132**, 1119–49. doi: [10.1130/B35178.1](https://doi.org/10.1130/B35178.1).
- Pawley MJ, Dutch RA and Wise TW** (2020) The relationship between crustal architecture, deformation, and magmatism in the Coompana Province, Australia. *Tectonics* **39**. doi: [10.1029/2019tc005593](https://doi.org/10.1029/2019tc005593).
- Plumb KA** (1991) New Precambrian time scale. *International Union of Geological Sciences* **14**, 139–40. doi: [10.18814/epiugs/1991/v14i2/005](https://doi.org/10.18814/epiugs/1991/v14i2/005).
- Plumb KA and James HL** (1986) Subdivision of precambrian time: recommendations and suggestions by the subcommission on precambrian stratigraphy. *Precambrian Research* **32**, 65–92. doi: [10.1016/0301-9268\(86\)90031-8](https://doi.org/10.1016/0301-9268(86)90031-8).
- Powell CM, Preiss WV, Gatehouse CG, Krapez B and Li Z-X** (1994) South Australian record of a Rodinian epicontinental basin and its mid-neoproterozoic breakup (~700 Ma) to form the Palaeo-Pacific Ocean. *Tectonophysics* **237**, 113–40. doi: [10.1016/0040-1951\(94\)90250-x](https://doi.org/10.1016/0040-1951(94)90250-x).
- Prave AR, Condon DJ, Hoffmann KH, Tapster S and Fallick AE** (2016) Duration and nature of the end-Cryogenian (Marinoan) glaciation. *Geology* **44**, 631–34. doi: [10.1130/G38089.1](https://doi.org/10.1130/G38089.1).
- Preiss WV** (1985) *Stratigraphy and Tectonics of the Worumba Anticline and Associated Intrusive Breccias*. Bulletin 52. Adelaide, South Australia: Geological Survey of South Australia.
- Preiss WV** (1987) *Adelaide Geosyncline—late Proterozoic stratigraphy, Sedimentation, Palaeontology and Tectonics*. Bulletin 53. Adelaide, South Australia: Geological Survey of South Australia. <https://sarigbasis.pir.sa.gov.au/WebtopEw/ws/samref/sarig1/wci/Record?r=0&m=1&w=catno=3147>
- Preiss WV** (1993) Neoproterozoic. In *The geology of South Australia Vol. 1 The Precambrian*, Bulletin 54 (eds JF Drexel, WV Preiss and AJ Parker), pp. 171–204. Adelaide, South Australia: Geological Survey of South Australia.
- Preiss WV** (2000) The Adelaide Geosyncline of South Australia and its significance in Neoproterozoic continental reconstruction. *Precambrian Research* **100**, 21–63. doi: [10.1016/S0301-9268\(99\)00068-6](https://doi.org/10.1016/S0301-9268(99)00068-6).
- Preiss WV** (2006) Old Boolcoomata Conglomerate member of the Benda Siltstone. *MESA Journal* **41**, 15–23. <https://sarigbasis.pir.sa.gov.au/WebtopEw/ws/samref/sarig1/wci/Record?r=0&m=1&w=catno=2025262>
- Preiss WV** (2014) *Geology and Mineral Resources of Bimbowrie Conservation Park – The MacDonald Corridor and Adjacent Parts of the Palaeo- to Mesoproterozoic Basement*. Report Book 2014/00003. South Australia: Geological Survey of South Australia, Department for Manufacturing, Trade, Resources and Energy. <https://sarigbasis.pir.sa.gov.au/WebtopEw/ws/samref/sarig1/wci/Record?r=0&m=1&w=catno=2036052>
- Preiss WV, Alexander EM, Cowley WM and Schwarz MP** (2002) Towards defining South Australia’s geological provinces and sedimentary basins. *MESA Journal* **27**, 39–52. <https://sarigbasis.pir.sa.gov.au/WebtopEw/ws/samref/sarig1/wci/Record?r=0&m=1&w=catno=2022981>
- Preiss WV and Conor CHH** (2001) Origin and nomenclature of the Wilyama Inliers, Curnamona Province. *MESA Journal* **21**, 47–9. <https://sarigbasis.pir.sa.gov.au/WebtopEw/ws/samref/sarig1/wci/Record?r=0&m=1&w=catno=2022263>
- Preiss WV, Drexel JF and Reid AJ** (2009) Definition and age of the Kooringa member of the Skillogelee Dolomite: host for Neoproterozoic (c. 790 Ma) porphyry related copper mineralisation at Burra. *MESA Journal* **55**, 19–33. <https://sarigbasis.pir.sa.gov.au/WebtopEw/ws/samref/sarig1/wci/Record?r=0&m=1&w=catno=2028895>
- Preiss WV, Dyson IA, Reid PW and Cowley WM** (1998) Revision of lithostratigraphic classification of the Umberatana Group. *MESA Journal* **9**, 36–42. <https://sarigbasis.pir.sa.gov.au/WebtopEw/ws/samref/sarig1/wci/Record?r=0&m=1&w=catno=2025009>
- Preiss WV, Gostin VA, McKirdy DM, Ashley PM, Williams GE and Schmidt PW** (2011) The glacial succession of Sturtian age in South Australia: The

- Yudnamutana Subgroup. In *The Geological Record of Neoproterozoic Glaciations* (eds E Arnaud, GP Halverson and GA Shields-Zhou), pp. 701–12: Geological Society, Memoirs 36. doi: [10.1144/M36.69](https://doi.org/10.1144/M36.69).
- Preiss WV, Walter MR, Coats RP and Wells AT (1978) Lithological correlations of Adelaidean glaciogenic rocks in parts of the Amadeus, Ngalia, and Georgina Basins. *AGSO Journal of Australian Geology and Geophysics* 3, 43–53. <http://pid.geoscience.gov.au/dataset/ga/80944>
- Rafiei M and Kennedy M (2019) Weathering in a world without terrestrial life recorded in the Mesoproterozoic Velkerri Formation. *Nature Communications* 10, 3448. doi: [10.1038/s41467-019-11421-4](https://doi.org/10.1038/s41467-019-11421-4).
- Rafiei M, Löhr S, Baldermann A, Webster R and Kong C (2020) Quantitative petrographic differentiation of detrital vs diagenetic clay minerals in marine sedimentary sequences: implications for the rise of biotic soils. *Precambrian Research* 350, 105948. doi: [10.1016/j.precamres.2020.105948](https://doi.org/10.1016/j.precamres.2020.105948).
- Redaa A, Farkaš J, Gilbert S, Collins AS, Wade B, Löhr S, Zack T and Garbe-Schönberg D (2021) Assessment of elemental fractionation and matrix effects during in situ Rb–Sr dating of phlogopite by LA-ICP-MS/MS: implications for the accuracy and precision of mineral ages. *Journal of Analytical Atomic Spectrometry* 36, 322–44. doi: [10.1039/d0ja00299b](https://doi.org/10.1039/d0ja00299b).
- Reid AJ, Halpin JA and Dutch RA (2019) Timing and style of high-temperature metamorphism across the Western Gawler Craton during the Paleo- to Mesoproterozoic. *Australian Journal of Earth Sciences* 66, 1085–111. doi: [10.1080/08120099.2019.1602565](https://doi.org/10.1080/08120099.2019.1602565).
- Reid AJ and Hand M (2012) Mesoarchean to Mesoproterozoic evolution of the southern Gawler Craton, South Australia. *Episodes* 35, 216–25. doi: [10.18814/epiiugs/2012/v35i1/021](https://doi.org/10.18814/epiiugs/2012/v35i1/021).
- Reid AJ, Hand M, Jagodzinski EA, Kelsey DE and Pearson NJ (2008) Paleoproterozoic orogenesis in the southeastern Gawler Craton, South Australia. *Australian Journal of Earth Sciences* 55, 449–71. doi: [10.1080/08120090801888594](https://doi.org/10.1080/08120090801888594)
- Reid AJ, Jagodzinski EA, Armit RJ, Dutch RA, Kirkland CL, Betts PG and Schaefer BF (2014a) U–Pb and Hf isotopic evidence for Neoproterozoic basement in the buried northern Gawler Craton, South Australia. *Precambrian Research* 250, 127–42. doi: [10.1016/j.precamres.2014.05.019](https://doi.org/10.1016/j.precamres.2014.05.019).
- Reid AJ, Jagodzinski EA, Fraser GL and Pawley MJ (2014b) SHRIMP U–Pb zircon age constraints on the tectonics of the Neoproterozoic to early Paleoproterozoic transition within the Mulgathing Complex, Gawler Craton, South Australia. *Precambrian Research* 250, 27–49. doi: [10.1016/j.precamres.2014.05.013](https://doi.org/10.1016/j.precamres.2014.05.013).
- Reid AJ, Jagodzinski EA, Wade CE, Payne JL and Jourdan F (2017) Recognition of c. 1780Ma magmatism and metamorphism in the buried northeastern Gawler Craton: correlations with events of the Aileron Province. *Precambrian Research* 302, 198–220. doi: [10.1016/j.precamres.2017.09.010](https://doi.org/10.1016/j.precamres.2017.09.010).
- Reid AJ and Payne JL (2017) Magmatic zircon Lu–Hf isotopic record of juvenile addition and crustal reworking in the Gawler Craton, Australia. *Lithos* 292–293, 294–306. doi: [10.1016/j.lithos.2017.08.010](https://doi.org/10.1016/j.lithos.2017.08.010).
- Reid AJ, Tiddy C, Jagodzinski E, Crowley J, Conor C, Brododewo A and Wade C (2021) *Precise zircon U–Pb Geochronology of Hiltaba Suite Granites, Point Riley, Yorke Peninsula*. Report Book 2021/00001. South Australia: Geological Survey of South Australia, Department for Energy and Mining. doi: [10.13140/RG.2.2.26820.96643](https://doi.org/10.13140/RG.2.2.26820.96643).
- Rooney AD, Chew DM and Selby D (2011) Re–Os geochronology of the Neoproterozoic–Cambrian Dalradian Supergroup of Scotland and Ireland: Implications for Neoproterozoic stratigraphy, glaciations and Re–Os systematics. *Precambrian Research* 185, 202–14. doi: [10.1016/j.precamres.2011.01.009](https://doi.org/10.1016/j.precamres.2011.01.009).
- Rooney AD, Macdonald FA, Strauss JV, Dudas FÖ, Hallmann C and Selby D (2014) Re–Os geochronology and coupled Os–Sr isotope constraints on the Sturtian snowball Earth. *Proceedings of the National Academy of Sciences of the United States of America* 111, 51–6. doi: [10.1073/pnas.1317266110](https://doi.org/10.1073/pnas.1317266110).
- Rooney AD, Strauss JV, Brandon AD and Macdonald FA (2015) A Cryogenian chronology: two long-lasting synchronous Neoproterozoic glaciations. *Geology* 43, 459–62. doi: [10.1130/G36511.1](https://doi.org/10.1130/G36511.1).
- Rooney AD, Yang C, Condon DJ, Zhu M and Macdonald FA (2020) U–Pb and Re–Os geochronology tracks stratigraphic condensation in the Sturtian snowball Earth aftermath. *Geology*. doi: [10.1130/G47246.1](https://doi.org/10.1130/G47246.1).
- Rose CV, Maloof AC, Schoene B, Ewing RC, Linnemann U, Hofmann M and Cottle JM (2013) PAUL F. HOFFMAN SERIES the end-Cryogenian Glaciation of South Australia. *Geoscience Canada* 40, 256–93. doi: [10.12789/geocanj.2013.40.019](https://doi.org/10.12789/geocanj.2013.40.019).
- Ross GM and Villeneuve J (1997) U–Pb geochronology of stranger stones in Neoproterozoic diamicrites, Canadian Cordillera: implications for provenance and ages of deposition. *Report 10*, pp. 141–55. Geological Survey of Canada, Natural Resources Canada. doi: [10.4095/209100](https://doi.org/10.4095/209100).
- Rubatto D (2002) Zircon trace element geochemistry: partitioning with garnet and the link between U–Pb ages and metamorphism. *Chemical Geology* 184, 123–38. doi: [10.1016/S0009-2541\(01\)00355-2](https://doi.org/10.1016/S0009-2541(01)00355-2).
- Rud'ko S, Kuznetsov N, Shatsillo A, Rud'ko D, Malyshev S, Dubenskiy A, Sheshukov V, Kanygina N and Romanyuk T (2020) Sturtian glaciation in Siberia: evidence of glacial origin and U–Pb dating of the diamicrites of the Chivida Formation in the north of the Yenisei Ridge. *Precambrian Research* 345. doi: [10.1016/j.precamres.2020.105778](https://doi.org/10.1016/j.precamres.2020.105778).
- Schmitz MD (2012) Radiometric ages used in GTS2012. In *The Geologic Time Scale* (eds FM Gradstein, JG Ogg, MD Schmitz and GM Ogg), pp. 1045–82. doi: [10.1016/b978-0-444-59425-9.15002-4](https://doi.org/10.1016/b978-0-444-59425-9.15002-4).
- Segnit RW (1939) *The Precambrian–Cambrian succession – The General and Economic Geology of These Systems, in Portions of South Australia*. Bulletin 18: Department of Mines. <https://sarigbasis.pir.sa.gov.au/WebtopEw/ws/samref/sarig1/wci/Record?r=0&m=1&w=catno=1009020>
- Shields GA, Halverson GP and Porter SM (2018) Descent into the Cryogenian. *Precambrian Research* 319, 1–5. doi: [10.1016/j.precamres.2018.08.015](https://doi.org/10.1016/j.precamres.2018.08.015).
- Shields GA, Strachan RA, Porter SM, Halverson GP, Macdonald FA, Plumb KA, de Alvarenga CJ, Banerjee DM, Bekker A, Bleeker W, Brasier A, Chakraborty PP, Collins AS, Condie K, Das K, Evans DAD, Ernst R, Fallick AE, Frimmel H, Fuck R, Hoffman PF, Kamber BS, Kuznetsov AB, Mitchell RN, Poiré DG, Poulton SW, Riding R, Sharma M, Storey C, Stueeken E, Tostevin R, Turner E, Xiao S, Zhang S, Zhou Y and Zhu M (2022) A template for an improved rock-based subdivision of the pre-Cryogenian timescale. *Journal of the Geological Society* 179. doi: [10.1144/jgs2020-222](https://doi.org/10.1144/jgs2020-222).
- Shields-Zhou GA, Porter SM and Halverson GP (2016) A new rock-based definition for the Cryogenian Period (Circa 720–635 Ma). *Episodes* 39. doi: [10.18814/epiiugs/2016/v39i1/89231](https://doi.org/10.18814/epiiugs/2016/v39i1/89231).
- Sláma J, Košler J, Condon DJ, Crowley JL, Gerdes A, Hanchar JM, Horstwood MSA, Morris GA, Nasdala L, Norberg N, Schaltegger U, Schoene B, Tubrett MN and Whitehouse MJ (2008) Plešovice zircon — a new natural reference material for U–Pb and Hf isotopic microanalysis. *Chemical Geology* 249, 1–35. doi: [10.1016/j.chemgeo.2007.11.005](https://doi.org/10.1016/j.chemgeo.2007.11.005).
- Smithies RH, Howard HM, Evins PM, Kirkland CL, Bodorkos S and Wingate MTD (2008) *The West Musgrave Complex – New geological Insights from Recent Mapping, Geochronology, and Geochemical Studies*. Record 2008/19: Geological Survey of Western Australia, Department of Industry and Resources. <http://dmpbookshop.eruditetechnologies.com.au/product/the-west-musgrave-complex-new-geological-insights-from-recent-mapping-geochronology-and-geochemical-studies.do>
- Smithies RH, Howard HM, Evins PM, Kirkland CL, Kelsey DE, Hand M, Wingate MTD, Collins AS and Belousova EA (2011) High-temperature granite magmatism, crust–mantle interaction and the Mesoproterozoic intracontinental evolution of the Musgrave Province, Central Australia. *Journal of Petrology* 52, 931–58. doi: [10.1093/petrology/egr010](https://doi.org/10.1093/petrology/egr010).
- Smits RG, Collins WJ, Hand M, Dutch R and Payne J (2014) A Proterozoic Wilson cycle identified by Hf isotopes in central Australia: implications for the assembly of Proterozoic Australia and Rodinia. *Geology* 42, 231–4. doi: [10.1130/g35112.1](https://doi.org/10.1130/g35112.1).
- Song G, Wang X, Shi X and Jiang G (2017) New U–Pb age constraints on the upper Banxi Group and synchrony of the Sturtian glaciation in South China. *Geoscience Frontiers* 8, 1161–73. doi: [10.1016/j.gsf.2016.11.012](https://doi.org/10.1016/j.gsf.2016.11.012).
- Sprigg RC (1952) Sedimentation in the Adelaide Geosyncline and the formation of the continental terrace. In *Sir Douglas Mawson Anniversary Volume* (eds MF Glaessner and RC Sprigg), pp. 153–9. Adelaide, South Australia: The University of Adelaide.
- Środoń J, Gerdes A, Kramers J and Bojanowski MJ (2022) Age constraints of the Sturtian glaciation on western Baltica based on U–Pb and Ar–Ar dating of

- the Lapichi Svita. *Precambrian Research* 371. doi: [10.1016/j.precamres.2022.106595](https://doi.org/10.1016/j.precamres.2022.106595).
- Stevens BPJ, Page RW and Crooks A** (2008) Geochronology of Willyama Supergroup metavolcanics, metasediments and contemporaneous intrusions, Broken Hill, Australia. *Australian Journal of Earth Sciences* 55, 301–30. doi: [10.1080/08120090701769456](https://doi.org/10.1080/08120090701769456).
- Strauss JV, Rooney AD, Macdonald FA, Brandon AD and Knoll AH** (2014) 740 Ma vase-shaped microfossils from Yukon, Canada: Implications for Neoproterozoic chronology and biostratigraphy. *Geology* 42, 659–62. doi: [10.1130/G35736.1](https://doi.org/10.1130/G35736.1).
- Subarkah D, Blades ML, Collins AS, Farkaš J, Gilbert S, Löhr SC, Redaa A, Cassidy E and Zack T** (2021) Unraveling the histories of Proterozoic shales through in situ Rb–Sr dating and trace element laser ablation analysis. *Geology*. doi: [10.1130/G49187.1](https://doi.org/10.1130/G49187.1).
- Subarkah D, Nixon AL, Jimenez M, Collins AS, Blades ML, Farkaš J, Gilbert SE, Holford S and Jarrett A** (2022) Constraining the geothermal parameters of in situ Rb–Sr dating on Proterozoic shales and their subsequent applications. *Geochronology* 4, 577–600. doi: [10.5194/gchron-4-577-2022](https://doi.org/10.5194/gchron-4-577-2022)
- Swain G, Woodhouse A, Hand M, Barovich K, Schwarz M and Fanning CM** (2005) Provenance and tectonic development of the late Archaean Gawler Craton, Australia; U–Pb zircon, geochemical and Sm–Nd isotopic implications. *Precambrian Research* 141, 106–36. doi: [10.1016/j.precamres.2005.08.004](https://doi.org/10.1016/j.precamres.2005.08.004).
- Thomson BP, Coats RP, Mirams RC, Forbes BG, Dalgarno CR and Johnson JE** (1964) Precambrian rock groups in the Adelaide Geosyncline: a new subdivision. *Quarterly Geological Notes* 9, 1–20.
- Tostevin R and Mills BJW** (2020) Reconciling proxy records and models of earth's oxygenation during the Neoproterozoic and Palaeozoic. *Interface Focus* 10, 20190137. doi: [10.1098/rsfs.2019.0137](https://doi.org/10.1098/rsfs.2019.0137).
- van der Wolff EJ** (2020) *Detrital provenance and geochronology of the Burra, Umberatana and Wilpena groups in the Mount Lofty Ranges*. Honours Thesis, Department of Earth Sciences, University of Adelaide, Adelaide, South Australia. Published thesis.
- Verdel C, Campbell MJ and Allen CM** (2021) Detrital zircon petrochronology of central Australia, and implications for the secular record of zircon trace element composition. *Geosphere*. doi: [10.1130/ges02300.1](https://doi.org/10.1130/ges02300.1).
- Vermeesch P** (2018) IsoplotR: a free and open toolbox for geochronology. *Geoscience Frontiers* 9. doi: [10.1016/j.gsf.2018.04.001](https://doi.org/10.1016/j.gsf.2018.04.001).
- Villa IM, De Bièvre P, Holden NE and Renne PR** (2015) IUPAC-IUGS recommendation on the half life of ⁸⁷Rb. *Geochimica et Cosmochimica Acta* 164, 382–5. doi: [10.1016/j.gca.2015.05.025](https://doi.org/10.1016/j.gca.2015.05.025).
- Virgo GM, Collins AS, Amos KJ, Farkaš J, Blades ML and Subarkah D** (2021) Descending into the “snowball”: High resolution sedimentological and geochemical analysis across the Tonian to Cryogenian boundary in South Australia. *Precambrian Research* 367. doi: [10.1016/j.precamres.2021.106449](https://doi.org/10.1016/j.precamres.2021.106449).
- Wade BP, Kelsey DE, Hand M and Barovich KM** (2008) The Musgrave Province: stitching north, west and south Australia. *Precambrian Research* 166, 370–86. doi: [10.1016/j.precamres.2007.05.007](https://doi.org/10.1016/j.precamres.2007.05.007).
- Wade CE** (2011) Definition of the Mesoproterozoic Ninnerie Supersuite, Curnamona Province, South Australia. *MESA Journal* 62, 25–42.
- Wade CE, McAvaney SO and Gordan GA** (2014) The Beda Basalt: new geochemistry, isotopic data and its definition. *MESA Journal* 73, 24–39.
- Wallace MW, Hood, Av, Shuster A, Greig A, Planavsky NJ and Reed CP** (2017) Oxygenation history of the Neoproterozoic to early Phanerozoic and the rise of land plants. *Earth and Planetary Science Letters* 466, 12–9. doi: [10.1016/j.epsl.2017.02.046](https://doi.org/10.1016/j.epsl.2017.02.046).
- Wallace MW, Hood AvS, Woon EMS, Giddings JA and Fromhold TA** (2015) The Cryogenian Balcanooona reef complexes of the Northern Flinders Ranges: implications for Neoproterozoic ocean chemistry. *Palaeogeography, Palaeoclimatology, Palaeoecology* 417, 320–36. doi: [10.1016/j.palaeo.2014.09.028](https://doi.org/10.1016/j.palaeo.2014.09.028).
- Wang D, Zhu X-K, Zhao N, Yan B, Li X-H, Shi F and Zhang F** (2019) Timing of the termination of Sturtian glaciation: SIMS U–Pb zircon dating from South China. *Journal of Asian Earth Sciences* 177, 287–94. doi: [10.1016/j.jseas.2019.03.015](https://doi.org/10.1016/j.jseas.2019.03.015).
- Webb AW** (1980) *Geochronology of Stratigraphically Significant Rocks from South Australia*. Progress Report No. 30. *Envelope Env* 01689, pp. 284–88. South Australia: Amdel Ltd., <https://sarigbasis.pir.sa.gov.au/WebtopEw/ws/samref/sarig1/wcir/Record?r=0&m=1&w=catno=2021979>
- Webb AW, Coats RP, Fanning CM and Flint RB** (1983) Geochronological framework of the Adelaide geosyncline. In *Adelaide Geosyncline Sedimentary Environments and Tectonics Settings Symposium*, pp. 7–9. Adelaide, South Australia: Geological Society of Australia, Abstracts 10.
- Wiedenbeck M, Allé P, Corfu F, Griffin WL, Meier M, Oberli F, Quadt AV, Roddick JC and Spiegel W** (1995) Three natural zircon standards for U–Th–Pb, Lu–Hf, trace element and REE analyses. *Geostandards Newsletter* 19, 1–23. doi: [10.1111/j.1751-908X.1995.tb00147.x](https://doi.org/10.1111/j.1751-908X.1995.tb00147.x).
- Wiedenbeck M, Hanchar JM, Peck WH, Sylvester P, Valley J, Whitehouse M, Kronz A, Morishita Y, Nasdala L, Fiebig J, Franchi I, Girard JP, Greenwood RC, Hinton R, Kita N, Mason PRD, Norman M, Ogasawara M, Piccoli PM, Rhede D, Satoh H, Schulz-Dobrick B, Skår O, Spicuzza MJ, Terada K, Tindle A, Togashi S, Vennemann T, Xie Q and Zheng YF** (2004) Further characterisation of the 91500 zircon crystal. *Geostandards and Geoanalytical Research* 28, 9–39. doi: [10.1111/j.1751-908X.2004.tb01041.x](https://doi.org/10.1111/j.1751-908X.2004.tb01041.x).
- Williams GE and Gostin VA** (2019) Late Cryogenian glaciation in South Australia: fluctuating ice margin and no extreme or rapid post-glacial sea-level rise. *Geoscience Frontiers*. doi: [10.1016/j.gsf.2019.02.002](https://doi.org/10.1016/j.gsf.2019.02.002).
- Wingate MTD, Campbell IH, Compston W and Gibson GM** (1998) Ion microprobe U–Pb ages for Neoproterozoic basaltic magmatism in south-central Australia and implications for the breakup of Rodinia. *Precambrian Research* 87, 135–59. doi: [10.1016/S0301-9268\(97\)00072-7](https://doi.org/10.1016/S0301-9268(97)00072-7).
- Wysockanski RJ and Allibone AH** (2004) Age, correlation, and provenance of the Neoproterozoic Skelton Group, Antarctica: Grenville age detritus on the margin of East Antarctica. *Journal of Geology* 112, 401–16. doi: [10.1086/421071](https://doi.org/10.1086/421071).
- Xu B, Xiao S, Zou H, Chen Y, Li Z-X, Song B, Liu D, Zhou C and Yuan X** (2009) SHRIMP zircon U–Pb age constraints on Neoproterozoic Quruqtagh diamictites in NW China. *Precambrian Research* 168, 247–58. doi: [10.1016/j.precamres.2008.10.008](https://doi.org/10.1016/j.precamres.2008.10.008).
- Young GM and Gostin VA** (1989a) Depositional environment and regional stratigraphic significance of the Serle Conglomerate: a Late Proterozoic submarine fan complex, South Australia. *Palaeogeography, Palaeoclimatology, Palaeoecology* 71, 237–52. doi: [10.1016/0031-0182\(89\)90052-7](https://doi.org/10.1016/0031-0182(89)90052-7).
- Young GM and Gostin VA** (1989b) An exceptionally thick upper Proterozoic (Sturtian) glacial succession in the Mount Painter area, South Australia. *Geological Society of America Bulletin* 101, 834–45. doi: [10.1130/0016-7606\(1989\)101<0834:Aetups>2.3.Co;2](https://doi.org/10.1130/0016-7606(1989)101<0834:Aetups>2.3.Co;2).
- Young GM and Gostin VA** (1991) Late Proterozoic (Sturtian) succession of the North Flinders Basin, South Australia; An example of temperate glaciation in an active rift setting. In *Glacial Marine Sedimentation; Paleoclimatic Significance*, (eds JB Anderson and GM Ashley), vol. 261, pp. 207–22. Geological Society of America. doi: [10.1130/SPE261-p207](https://doi.org/10.1130/SPE261-p207)
- Zaitseva TS, Kuznetsov AB, Gorozhanin VM, Gorokhov IM, Ivanovskaya TA and Konstantinova GV** (2019) The lower boundary of the Vendian in the Southern Urals as evidenced by the Rb–Sr age of Glauconites of the Bakeevo Formation. *Stratigraphy and Geological Correlation* 27, 573–87. doi: [10.1134/s0869593819050083](https://doi.org/10.1134/s0869593819050083).
- Zhang Q-R, Li X-H, Feng L-J, Huang J and Song B** (2008) A new age constraint on the onset of the Neoproterozoic glaciations in the Yangtze Platform, South China. *The Journal of Geology* 116, 423–9. doi: [10.1086/589312](https://doi.org/10.1086/589312).
- Zhang S, Jiang G, Zhang J, Song B, Kennedy MJ and Christie-Blick N** (2005) U–Pb sensitive high-resolution ion microprobe ages from the Doushantuo Formation in south China: constraints on late Neoproterozoic glaciations. *Geology* 33, 473–76. doi: [10.1130/g21418.1](https://doi.org/10.1130/g21418.1).
- Zhou C-M, Huyskens MH, Xiao S and Yin Q-Z** (2020) Refining the termination age of the Cryogenian Sturtian glaciation in South China. *Palaeoworld* 29, 462–8. doi: [10.1016/j.palwor.2020.04.002](https://doi.org/10.1016/j.palwor.2020.04.002).
- Zhou C, Huyskens MH, Lang X, Xiao S and Yin Q-Z** (2019) Calibrating the terminations of Cryogenian global glaciations. *Geology* 47, 251–4. doi: [10.1130/g45719.1](https://doi.org/10.1130/g45719.1).
- Zhou C, Tucker R, Xiao S, Peng Z, Yuan X and Chen Z** (2004) New constraints on the ages of Neoproterozoic glaciations in south China. *Geology* 32, 437–40. doi: [10.1130/G20286.1](https://doi.org/10.1130/G20286.1).